


RESEARCH PAPER

Hydrogen sulfide regulates muscle RING finger-1 protein S-sulphydration at Cys⁴⁴ to prevent cardiac structural damage in diabetic cardiomyopathy

Xiaojiao Sun^{1*}  | Dechao Zhao^{2*} | Fangping Lu¹ | Shuo Peng¹ | Miao Yu¹ | Ning Liu¹ | Yu Sun¹ | Haining Du¹ | Bingzhu Wang¹ | Jian Chen¹ | Shiyun Dong¹ | Fanghao Lu¹ | Weihua Zhang^{1,3}

¹Department of Pathophysiology, Harbin Medical University, Harbin, China

²Department of Cardiology, First Affiliated Hospital of Harbin Medical University, Harbin, China

³Key Laboratory of Cardiovascular Medicine Research, Harbin Medical University Ministry of Education, Harbin, China

Correspondence

Weihua Zhang and Fanghao Lu, Department of Pathophysiology, Harbin Medical University, Harbin 150086, China.

Email: zhangwh116@126.com; lufanghao1973@126.com

Funding information

National Natural Science Foundation of China, Grant/Award Numbers: 81570340 and 81670344

Background and Purpose: Hydrogen sulfide (H₂S) plays important roles as a gasotransmitter in pathologies. Increased expression of the E3 ubiquitin ligase, muscle RING finger-1 (MuRF1), may be involved in diabetic cardiomyopathy. Here we have investigated whether and how exogenous H₂S alleviates cardiac muscle degradation through modifications of MuRF1 S-sulphydration in db/db mice.

Experimental Approach: Neonatal rat cardiomyocytes were treated with high glucose (40 mM), oleate (100 μM), palmitate (400 μM), and NaHS (100 μM) for 72 hr. MuRF1 was silenced with siRNA technology and mutation at Cys⁴⁴. Endoplasmic reticulum stress markers, MuRF1 expression, and ubiquitination level were measured. db/db mice were injected with NaHS (39 μmol·kg⁻¹) for 20 weeks. Echocardiography, cardiac ultrastructure, cystathionine-γ-lyase, cardiac structure proteins expression, and S-sulphydration production were measured.

Key Results: H₂S levels and cystathionine-γ-lyase protein expression in myocardium were decreased in db/db mice. Exogenous H₂S reversed endoplasmic reticulum stress, including impairment of the function of cardiomyocytes and structural damage in db/db mice. Exogenous H₂S could suppress the levels of myosin heavy chain 6 and myosin light chain 2 ubiquitination in cardiac tissues of db/db mice, and MuRF1 was modified by S-sulphydration, following treatment with exogenous H₂S, to reduce the interaction between MuRF1 and myosin heavy chain 6 and myosin light chain 2.

Conclusions and Implications: Our findings suggest that H₂S regulates MuRF1 S-sulphydration at Cys⁴⁴ to prevent myocardial degradation in the cardiac tissues of db/db mice.

Abbreviations: 4-PBA, sodium phenylbutyrate; C-7Az, 7-azido-4-methylcoumarin; CSE, cystathionine-γ-lyase; DCM, diabetic cardiomyopathy; EF, ejection fraction; ER, endoplasmic reticulum; FS, fractional shortening; HG, high glucose; KEGG, Kyoto Encyclopedia of Genes and Genomes; MuRF1, muscle RING finger-1; MYH6, myosin heavy chain 6; MyL2, myosin light chain 2; NRCMs, neonatal rat cardiomyocytes; Ole, oleate; Pal, palmitate; PPG, propylene glycol; PYR41, 4[4-(5-nitro-furan-2-ylmethylene)-3,5-dioxo-pyrazolidin-1-yl]-benzoic acid ethyl ester; SSP, SSP4 (3', 6'-di(O-thiosalicyl)fluorescein); UPR, unfolded protein response

*These authors contributed equally to this work.

LINKED ARTICLES: This article is part of a themed section on Hydrogen Sulfide in Biology & Medicine. To view the other articles in this section visit <http://onlinelibrary.wiley.com/doi/10.1111/bph.v177.4/issuetoc>

1 | INTRODUCTION

The prevalence of diabetes mellitus in the world has increased in the past 20 years and is currently estimated at 9% in the adult population. Patients with diabetes have a twofold to fourfold increased risk of suffering heart disease (Danaei et al., 2011). Increased free fatty acids and hyperglycaemia enhance malignant effects on the heart, causing cardiac dysfunction and structural damage that together constitute a distinct disease state, called diabetic cardiomyopathy (DCM; From et al., 2006; Sorrentino et al., 2017). Diabetic hearts have to increase fatty acid oxidation to maintain ATP production, which is accompanied by enhanced ROS generation and the ROS have adverse effects on cardiac functions (Ni et al., 2016). The main pathophysiological feature of DCM includes a shift in metabolic substrates at the early stage followed by increased ROS generation and induced structural damage, leading to end-stage cardiac diastolic and systolic dysfunction (Zhao & Yang, 2017).

The protein muscle RING finger-1 (MuRF1) is a ubiquitin ligase initially identified for its role in the regulation of skeletal muscle atrophy and cardiomyopathy (Bodine et al., 2001). MuRF1 is expressed in striated muscle specifically and is limited to the M-line and cytoplasm of cardiomyocytes, which have been found to degrade sarcomere proteins, including troponin I, troponin T, and titin (Centner et al., 2001). Several studies have demonstrated that increased ROS production increases MuRF1 expression, which is associated with the degradation of skeletal muscle (Maejima et al., 2014; Sato, Asano, Isono, Ito, & Asano, 2014; Sha et al., 2014).

Hydrogen sulfide (H₂S) has been widely recognized in recent years as having physiological importance as an endogenous gas and is accepted as the third gasotransmitter after NO and carbon monoxide (Calvert, Coetzee, & Lefer, 2010; Fu et al., 2012). Increasing evidence suggests that H₂S is involved in a wide range of physiological and pathological processes in the cardiovascular system, such as regulation of BP and reduced production of myocardial ROS (Stubbert et al., 2014; Untereiner et al., 2016). Our previous study showed that exogenous H₂S could facilitate the clearance of ubiquitin aggregates by promoting autophagy, which contributed to its antioxidative effects in DCM (J. Wu et al., 2017). Nevertheless, the pathogenesis of DCM is complex, and the precise mechanism by which H₂S may protect against DCM has not been thoroughly elucidated (Popov, 2013). To date, no information exists on the possible role of H₂S in protecting the intact cardiac structure in DCM. The aim of the present study was to investigate whether H₂S can modulate MuRF1 S-sulfhydration to attenuate the cardiac structural damage occurring in DCM.

What is already known

- The E3 ubiquitin ligase MuRF1 plays a critical role in the regulation of cardiomyopathy.

What this study adds

- H₂S regulates MuRF1 S-sulfhydration at Cys⁴⁴ to prevent myocardial degradation in db/db mice.

What is the clinical significance

- Increased S-sulfhydration of MuRF1 by H₂S may be a useful therapeutic strategy in diabetic cardiomyopathy.

2 | METHODS

2.1 | Experimental animals

All animal care and experimental procedures complied with the guidelines of China National Institute of Health (http://www.most.gov.cn/fggw/zfwj/zfwj2006/200609/t20060930_54389.htm) and were approved by the Animal Ethical Committee of Harbin Medical University. Animal studies are reported in compliance with the ARRIVE guidelines (Kilkenny, Browne, Cuthill, Emerson, & Altman, 2010) and with the recommendations made by the British Journal of Pharmacology. Female, leptin receptor-deficient (db/db) mice (RRID: IMSR_JAX:000697) on a C57BL/6 (RRID:MGI:5657888) background ($n = 90$, 8–10 weeks old) and their corresponding wild-type littermates ($n = 30$) were purchased from the Animal Model Institute of Nanjing (Nanjing, China). The animals were housed under diurnal lighting conditions (12h light and 12h dark) and fed standard mouse chow and water throughout the study period. Half of the db/db mice and their wild-type littermates were treated with NaHS (39 $\mu\text{mol}\cdot\text{kg}^{-1}$; i.p.) every 2 days for 20 weeks (Yang et al., 2008).

2.2 | Echocardiography analysis

Cardiac functions of mice were assessed using an echocardiography system (GE VIVID7 10S, St. CT., Fairfield, USA) after 6, 12, and 20 weeks of treatment by NaHS. Mice were lightly anaesthetized with tribromoethanol (Avertin; 240 $\text{mg}\cdot\text{kg}^{-1}$, i.p.) and the mouse body temperature was maintained as close to 37°C as possible during the entire

process (Papaioannou & Fox, 1993). Left ventricular parameters were measured including ejection fraction (EF, %) and fractional shortening (FS, %).

2.3 | Transmission electron microscopy

The mice were killed with an overdose of anaesthetic and left ventricular cardiac tissues were collected and fixed in 2.5% glutaraldehyde in 0.1-M sodium phosphate buffer (pH 7.3) at 4°C overnight and then treated with 1% osmium tetroxide for 2 hr. The left ventricular cardiac tissues were stained en bloc with saturated uranyl acetate for 1 hr and dehydrated in ethanol, embedded in epoxy resin. Ultrathin sections were cut on a Reichert Ultracut (Leica, Nussloch, Germany), and the ultrathin sections were stained with uranyl acetate and lead citrate by standard methods. All ultrastructural analyses were performed in a blinded and non-biased manner from photomicrographs captured using the Philips CM120 electron microscope.

2.4 | Staining of F-actin

To assess the integrity of myocardial fibres, cardiac tissues were stained with phalloidin (Solarbio, China; Watkins, Borthwick, & Arthur, 2011). Briefly, hearts were washed with cold PBS to remove blood and then frozen in cold isopentane and stored at -80°C for less than a week. Frozen sections (5–10 µm) were incubated with 20-µM phalloidin in PBS for 30 min and were then washed three times with PBS. The nuclei were labelled with DAPI (1:1,000, Solarbio, China). Visualization of filamentous actin (F-actin) in the frozen sections of mouse hearts was carried out using a fluorescence microscope (Olympus, XSZ-D2, Tokyo, Japan) with excitation by a 495 nm laser.

2.5 | Measurement of H₂S level in cardiac tissues

The levels of H₂S in the frozen cardiac tissues were determined by fluorescence, using 7-azido-4-methylcoumarin (C-7Az; Sigma, St Louis, MO), which is known to respond selectively to H₂S (B. Chen et al., 2013). Cardiac tissues were incubated with 50-µmol·L⁻¹ C-7Az PBS for 30 min followed by washing with PBS three times. Visualization of the turn-on fluorescence response of C-7Az to H₂S in cardiac tissues was implemented using fluorescence microscopy with the excitation of a 720 nm laser. These results confirmed that excitation fluorescence imaging could be used to detect H₂S through the triggered fluorescence response of C-7Az.

2.6 | Immunohistochemistry

The antibody-based procedures used here comply with the recommendations made by the *British Journal of Pharmacology*. Isolated cardiac tissues from db/db mice and wild-type mice were washed with PBS and fixed in 4% paraformaldehyde overnight before being embedded in paraffin. Embedded left ventricles were cut into 4 µm sections

to demonstrate the structure of the cardiac muscle. Sections were stained with haematoxylin/eosin for the detection of morphology.

2.7 | Culture of neonatal rat cardiomyocytes and treatment

Neonatal rat cardiomyocytes (NRCMs) were isolated from 1- to 3-day-old Sprague Dawley rats (RRID:RGD_70508) by enzymic digestion with 0.25% trypsin (Sigma). Briefly, neonatal Sprague Dawley rats was anaesthetized (isoflurane) and fixed on a platform, the skin disinfected with a medical cotton ball, soaked in 75% medical alcohol. The whole heart was excised and placed in cold PBS, washing to remove the blood. The left heart was isolated, cut into pieces and the pieces of cardiac tissue were digested with 0.25% trypsin in a water bath at 37°C for 5–10 min. This step of digestion was repeated eight times. Finally, the digestion was terminated by adding the same volume of DMEM (HyClone, USA) containing 10% FBS (NQBB, Australia). The mixture containing NRCMs was centrifuged in 1,000× *g* at 4°C for 10 min, the supernatant removed and the cell pellet resuspended in medium. The cell suspension was then allowed to attach for 1.5 hr and the non-attached cells (NRCMs) were washed off and collected. The NRCMs were plated onto 35-mm dishes at a density of 1 × 10⁶ cells·ml⁻¹ for a monolayer and cultured in low glucose (5.56 mM) DMEM (HyClone) containing 10% FBS (NQBB) and 100-units·ml⁻¹ penicillin/streptomycin for 72 hr before use. The cultured NRCMs were randomly divided into several groups as follows: control (low glucose, 5.5 mM), high glucose (HG; 40 mM) + **palmitate** (Pal, 400 µM) + **oleate** (Ole, 100 µM), HG + Pal + Ole + NaHS (100 µM), HG + Pal + Ole + PPG (10 nM, an irreversible competitive **cystathionine-γ-lyase [CSE]** inhibitor), HG + Pal + Ole + N-acetyl cysteine (NAC; 100 µM, an inhibitor of ROS), HG + Pal + Ole + **MG132** (20 µM, an inhibitor of proteasome activity), HG + Pal + Ole + NaHS + DTT (20 µM, an inhibitor of disulfide bonds), HG + Pal + Ole + PYR41 (3 µM, an inhibitor of ubiquitin-activating enzyme [E1]), HG + Pal + Ole + 4-PBA (5 mM, an inhibitor of endoplasmic reticulum [ER] stress), and control + **thapsigargin** (100 µM, an inducer of ER stress). Drugs were added directly into the culture for 48 hr. NRCMs were treated with HG, palmitate and oleate to model the cardiomyocytes under conditions of hyperglycaemia and hyperlipidaemia, as in diabetes.

2.8 | ROS level analysis

The NRCMs were treated with HG (40 mM) + Pal (400 µM) + Ole (100 µM), HG + Pal + Ole + NaHS (100 µM), HG + Pal + Ole + PPG (10 nM), or HG + Pal + Ole + NAC (100 µM) for 2, 4, 8, and 12 hr, respectively. The production of ROS was measured by DHE or DCFH. Briefly, the NRCMs were inoculated into 24-well plate and treated under different conditions. The NRCMs were washed with PBS three times and then incubated (45 min, 37°C, in the dark) in serum-free media containing DHE (25 µM) or DCFH (10 µM). After incubation,

NRCMs were washed and the DHE or DCFH retained was detected with a fluorescence microscope (Olympus, XSZ-D2).

2.9 | Western blotting

NRCMs or heart tissues were lysed in cell lysis buffer (Beyotime, Shanghai, China) or RIPA (Beyotime) separately, containing 1% PMSF. The protein lysates were centrifuged at 4°C, 12,000× *g* for 30 min. The supernatant was collected, and the protein concentration of each sample was evaluated by the BCA Protein Assay kit (Beyotime). Proteins were separated by SDS-PAGE and then transferred onto PVDF membranes (Millipore). After blocking with 5% BSA at room temperature, the membranes were blotted with primary antibodies overnight at 4°C as follows: rabbit-anti-CSE (ProteinTech group, 12217-1-AP, 1:500, RRID:AB_2087497), rabbit-anti-ATF4 (ProteinTech group, 10835-1-AP, 1:1000, RRID:AB_2058600), rabbit-anti-Bip (ProteinTech group, 11587-1-AP, 1:1000, RRID:AB_2119855), rabbit-anti-CHOP (ProteinTech group, 15204-1-AP, 1:1000, RRID:AB_2292610), rabbit-anti-p-PERK (Santa Cruz Biotechnology, sc32577, 1:500, RRID:AB_2293243), rabbit-anti-PERK (ProteinTech group, 20582-1-AP, 1:1000, RRID:AB_10695760), rabbit-anti-p-eIF2 α (Cell Signaling Technology, 3398S, 1:1000, RRID:AB_2096481), rabbit-anti-eIF2 α (ProteinTech group, 11233-1-AP, 1:1000, RRID:AB_2246321), rabbit-anti-myosin heavy chain 6 (MYH6; ProteinTech group, 22281-1-AP, 1:1000, RRID:AB_2736822), rabbit-anti-myosin light chain 2 (MyL2; ProteinTech group, 10906-1-AP, 1:1000, RRID:AB_2147453), rabbit-anti-MuRF1 (ProteinTech group, 55456-1-AP, RRID:AB_11232209, 1:1000), and rabbit-anti-ubiquitin (ProteinTech group, 10201-2-AP, 1:1000, RRID:AB_671515). β -Tubulin (ProteinTech group, 10068-1-AP, 1:1000, RRID:AB_2303998) was used as control. Membranes were washed with PBS three times and then incubated with the corresponding secondary antibodies at a 1:5,000 dilution for 1.5 hr at room temperature. The specific complex was visualized using ECL plus luminescent image analyser (ProteinSample).

2.10 | S-sulfhydration assay

S-sulfhydration was performed as described previously (Meng, Zhao, Xie, Han, & Ji, 2018). Briefly, NRCMs or heart tissues were homogenized in HEN buffer (composition; 250-mM HEPES-NaOH, pH 7.7: 1-mM EDTA; 0.1-mM neocuproine), supplemented with 100-mM deferoxamine and centrifuged at 13,000× *g* for 30 min at 4°C. NRCMs or heart tissue lysates were added to blocking buffer (HEN buffer with 2.5% SDS and 20-mM methyl methanethiosulfonate) at 50°C for 60 min with frequent vortexing. Methyl methanethiosulfonate was later removed by acetone, and the proteins were precipitated at -20°C for 60 min. After acetone removal, proteins were resuspended in HENS buffer (HEN buffer with 1% SDS). To the suspension was added 4-mM *N*-[6-(biotinamido)hexyl]-3-(2-pyridylthio)propionamide (biotin-HPDP) in DMSO without ascorbic acid. After incubation for 3 hr at 25°C, biotinylated proteins were precipitated by streptavidin-agarose beads, which were later washed with HENS

buffer. The biotinylated proteins were eluted by SDS-PAGE and subjected to Western blotting analysis using antibodies against MuRF1.

2.11 | Measurement of intracellular levels of polysulfide

Intracellular production of polysulfide was monitored using a newly developed fluorescent probe, SSP4, with slight modifications (Kimura et al., 2015). Briefly, NRCMs were loaded with 50- μ M SSP4 in a serum-free DMEM containing 0.003% Cremophor EL for 15 min at 37°C in the dark. After being washed, SSP4 was detected using the fluorescence microscope (Olympus, XSZ-D2).

2.12 | Immunoprecipitation

Briefly, NRCMs or heart tissue lysates were diluted to a concentration of 2 mg·ml⁻¹. About 500 μ g per sample of protein was used for immunoprecipitation. Protein A/G magnetic beads for immunoprecipitation were conjugated with rabbit-anti-MuRF1 antibody (10- μ g antibody per 500- μ g protein) and incubated with NRCMs or heart tissue lysates overnight at 4°C with gentle rotation. Beads were collected using centrifugation at 4°C, 10,000× *g* for 5 min, and beads were washed with cell lysis buffer containing 1% PMSF, three times. The precipitates were diluted with loading buffer and boiled for 10 min at 100°C and later used for Western blotting analyses to detect potential interacting proteins.

2.13 | siRNA transfection

NRCMs were treated according to the manufacturer's instructions with MuRF1 small-interfering RNA (siRNA; mouse; Sangon Biotech, China) for 48 hr to inhibit MuRF1 expression. NRCMs (70% confluent) were seeded in six-well plates, incubated with DMEM containing 10% FBS without penicillin/streptomycin. Transfection of NRCMs by siRNA was achieved using Lipofectamine RNAi MAX (Invitrogen). In brief, MuRF1 siRNA with the transfection reagent was incubated for 15 min to form complexes, which were subsequently added to plates containing cells and medium. The cells were incubated at 37°C in a CO₂ incubator for further analysis.

2.14 | LC-MS/MS analysis

To identify the lysine ubiquitylome of three cardiac tissues of db/db mice after the treatment of NaHS, the above extracted proteins were digested with proteases and later subjected to Kub peptide enrichment. To enrich Kub peptide, tryptic peptides dissolved in NETN buffer (100-mM NaCl, 1-mM EDTA, 50-mM Tris-HCl, 0.5% NP-40, pH 8.0) were incubated with pre-washed antibody beads (PTM Biolabs) at 4°C overnight with gentle shaking. The beads were washed four times with NETN buffer and twice with double-distilled H₂O. The bound peptides were eluted from the beads with 0.1% TFA. The eluted fractions were combined and vacuum-dried. The resulting

peptides were cleaned with C18 ZipTip (Millipore) according to the manufacturer's instructions followed by LC-MS/MS analysis (Pang et al., 2015; Yu et al., 2014). The resulting peptides were then analysed by nano-HPLC-MS/MS on a Q Exactive mass spectrometer (Thermo Fisher Scientific). Minimum peptide length was set to 7. All of the other parameters in MaxQuant were set to default values. The site localization probability was set as >0.75.

2.15 | Bioinformatic analysis

Pathway and functional annotation enrichment was performed using DAVID bioinformatics resources (RRID:SCR_001881). Cellular localization of identified proteins was further analysed on the basis of information available from Gene Ontology (<http://www.geneontology.org/>). Biological function classifications and signalling pathway analysis were performed with the tools on DAVID Bioinformatics Resources 2011 (<http://david.abcc.ncifcrf.gov/>). All statistics reported are Benjamini-Hochberg corrected *P* values. Molecular function categorization was performed using PANTHER (RRID:SCR_004869). Statistical analysis of enriched motifs was performed using motif-x. Network analysis was performed using Ingenuity Pathway Analysis (RRID:SCR_008653).

2.16 | Computational method

To date, the three-dimensional structure of MuRF1 has not been resolved; therefore, homology modelling, a promising tool to predict protein structure based on a template containing similar sequence, was applied in this study using Phyre2. The sequence of MuRF1 was obtained from Uniprot (RRID:SCR_002380). According to a sequence alignment by BLAST (RRID:SCR_004870), the crystal structure and active site of MuRF1 were calculated by the website of protein plus (RRID:SCR_005375).

2.17 | Point mutation of MuRF1

Adenoviruses expressing GFP and MuRF1-GFP were purchased from Cyagen Biosciences Inc. (Guangzhou, China). The full-length mouse MuRF1 with a single mutation of Cys⁴⁴ to alanine, and GFP cDNA was inserted into pM vector (Cyagen Biosciences) between the Kozak and T2A sites. The adenovirus was added directly to NRCMs, and after 4–6 hr for transfection, new fresh medium was added. The NRCMs were treated in different conditions 24 hr after transfection, and the related proteins were detected by Western blotting.

2.18 | Data and statistical analysis

The data and statistical analysis comply with the recommendations of the *British Journal of Pharmacology* on experimental design and analysis in pharmacology. All data are presented as the mean ± SD. Data were analysed using one-way ANOVA test followed by Bonferroni post hoc tests, as appropriate. The threshold of *P* < 0.05 was designated

statistically significant for all tests. All statistical analyses were performed using Prism 5 (GraphPad, La Jolla, CA, USA; RRID:SCR_002798).

2.19 | Materials

Compounds used in these experiments were supplied as follows: 4-PBA, biotin-HPDP, deferoxamine, NAC, NaHS, MG-132, oleate, palmitate, PPG, PYR41, thapsigargin and tribromoethanol were from Sigma (St Louis, MO). SSP was supplied by Dojindo Molecular Technologies Inc. (Rockville, MD). DHE and DHCF were supplied by Boster (Wuhan, China).

2.20 | Nomenclature of targets and ligands

Key protein targets and ligands in this article are hyperlinked to corresponding entries in <http://www.guidetopharmacology.org>, the common portal for data from the IUPHAR/BPS Guide to PHARMACOLOGY (Harding et al., 2018), and are permanently archived in the Concise Guide to PHARMACOLOGY 2017/18 (Alexander et al., 2017).

3 | RESULTS

3.1 | Exogenous H₂S improves DCM in db/db mice

To investigate the effects of H₂S on DCM, the ratio of heart weight/body weight and blood glucose level were measured. We found that the ratio of heart weight/body weight and blood glucose level both significantly increased in db/db mice compared with those in db/db + NaHS after 20 weeks (Tables S1–S3). To further characterise the effects of H₂S on cardiac function, we used echocardiography and found that EF and FS decreased at 12 and 20 weeks in db/db mice, whereas they were improved after treatment with NaHS (Figure 1a). The transmission electron microscopy assay indicated that exogenous H₂S reduced the degradation of cardiac sarcomeres compared with those in db/db mice at 12 and 20 weeks (Figures 1b and S1). To further confirm the effect of H₂S on cardiac structure, we assayed F-actin through phalloidin staining (green). The results showed that F-actin was degraded in db/db mice and exogenous H₂S prevented this degradation (Figure 1c). These results indicate that exogenous H₂S exerted protective effects against DCM.

3.2 | H₂S level and CSE expression in db/db mice

The levels of H₂S and CSE expression declined in db/db mice (Sun et al., 2018; J. Wu et al., 2017). The results showed that H₂S level and expression of CSE were reduced at 12 and 20 weeks in db/db mice but there was no significant change at 6 weeks, as shown C-7Az probe staining and Western blotting, respectively (Figure 2). Exogenous H₂S enhanced the H₂S level and CSE expression in the hearts of db/db mice, demonstrating that the change in H₂S is relevant to the maintenance of cardiac structure.

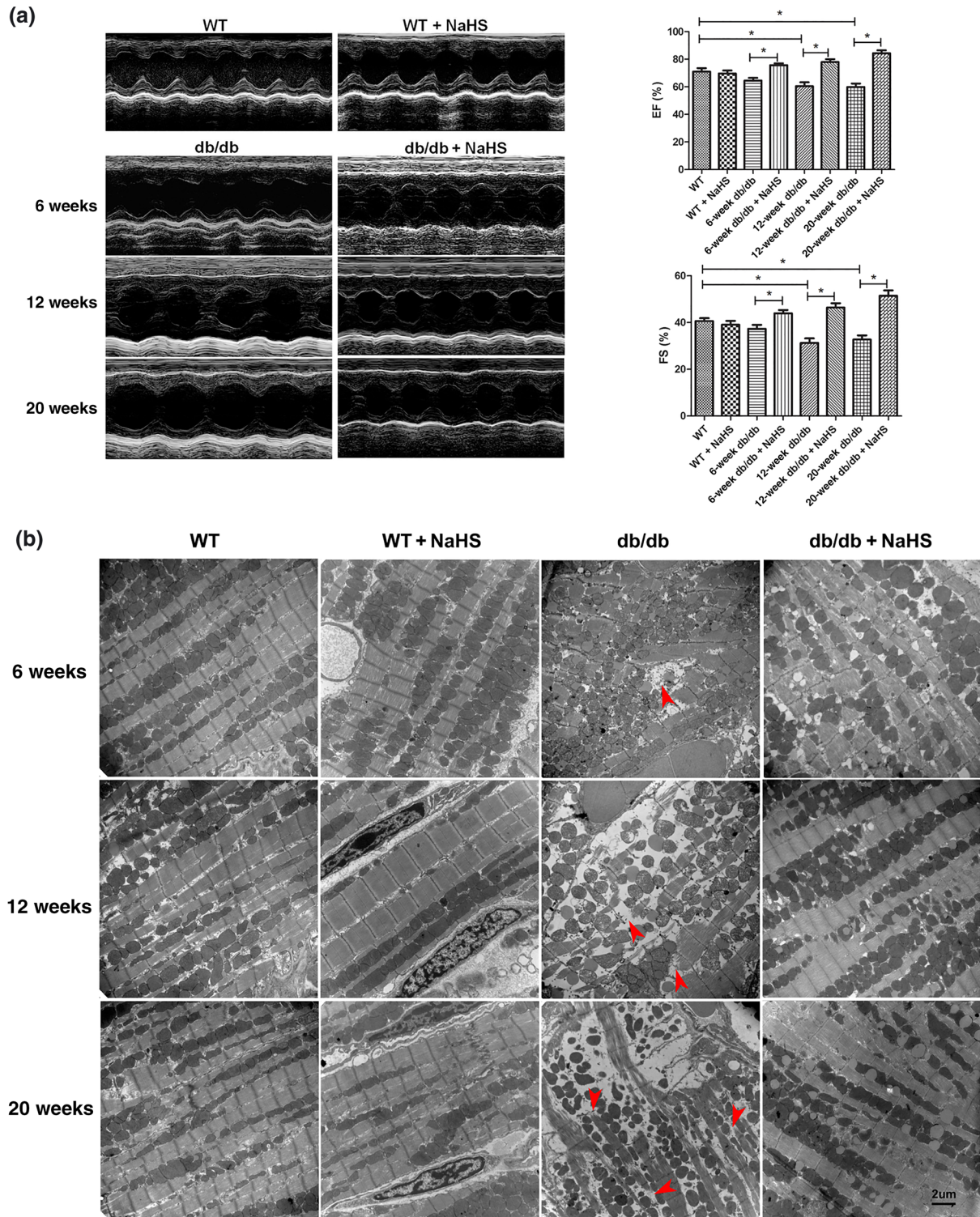


FIGURE 1 Exogenous H_2S protected cardiac function and cardiac ultrastructure in db/db mice. Female db/db mice and their wild-type littermates were injected with NaHS ($39 \mu\text{mol}\cdot\text{kg}^{-1}$) or saline every 2 days for 20 weeks. (a) Representative M-mode echocardiograms of hearts (left) and quantitative analysis of EF and FS by echocardiography (right) at 6, 12, and 20 weeks treated with NaHS are shown. (b) Cardiac ultrastructure of mice was examined with transmission electron microscope at 6, 12, and 20 weeks treated with NaHS. Bar = $2 \mu\text{m}$. (c) Cardiac structure was detected by phalloidin staining (green) of F-actin at 6, 12, and 20 weeks treated with NaHS. Data shown are means \pm SD; $n = 8$, $*P < 0.05$, significantly different as indicated; one-way ANOVA

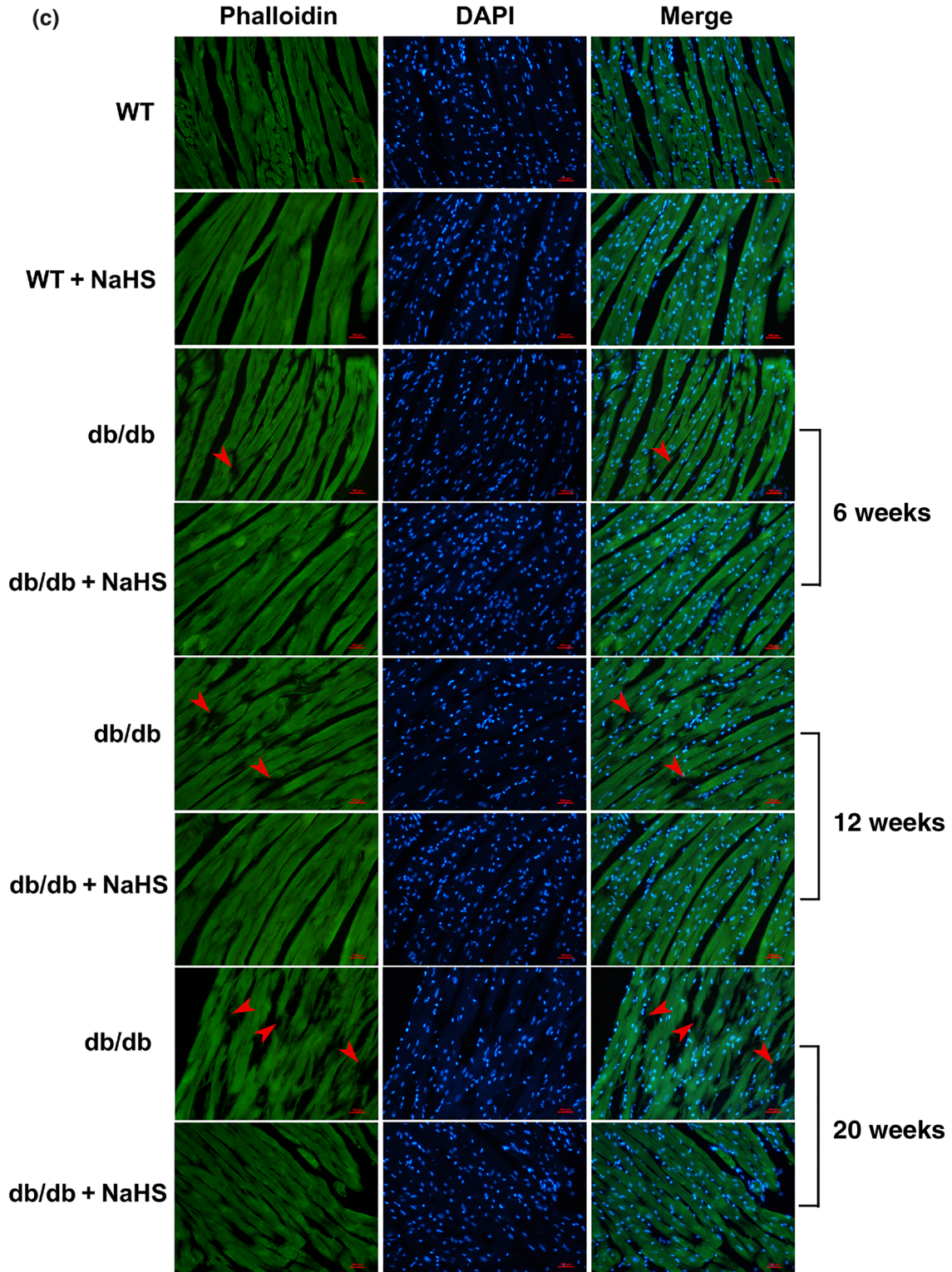


FIGURE 1 Continued.

3.3 | Exogenous H₂S ameliorated ER stress in vivo and in vitro

It is well known that H₂S has antioxidant effects. NRCMs were cultured with HG, palmitate and oleate to model the hyperglycaemia and hyperlipidaemia of Type 2 diabetes (S. Li et al., 2016). Under these

conditions, we assayed ROS production in NRCMs, using DHE and DCFH-DA staining. Production of ROS increased in the HG + Pal + Ole group compared with the control group. Exogenous H₂S and NAC (another antioxidant) reduced ROS production, while the CSE inhibitor, PPG, up-regulated ROS production (Figure S2). To investigate whether H₂S could suppress ER stress in db/db mice, we measured the

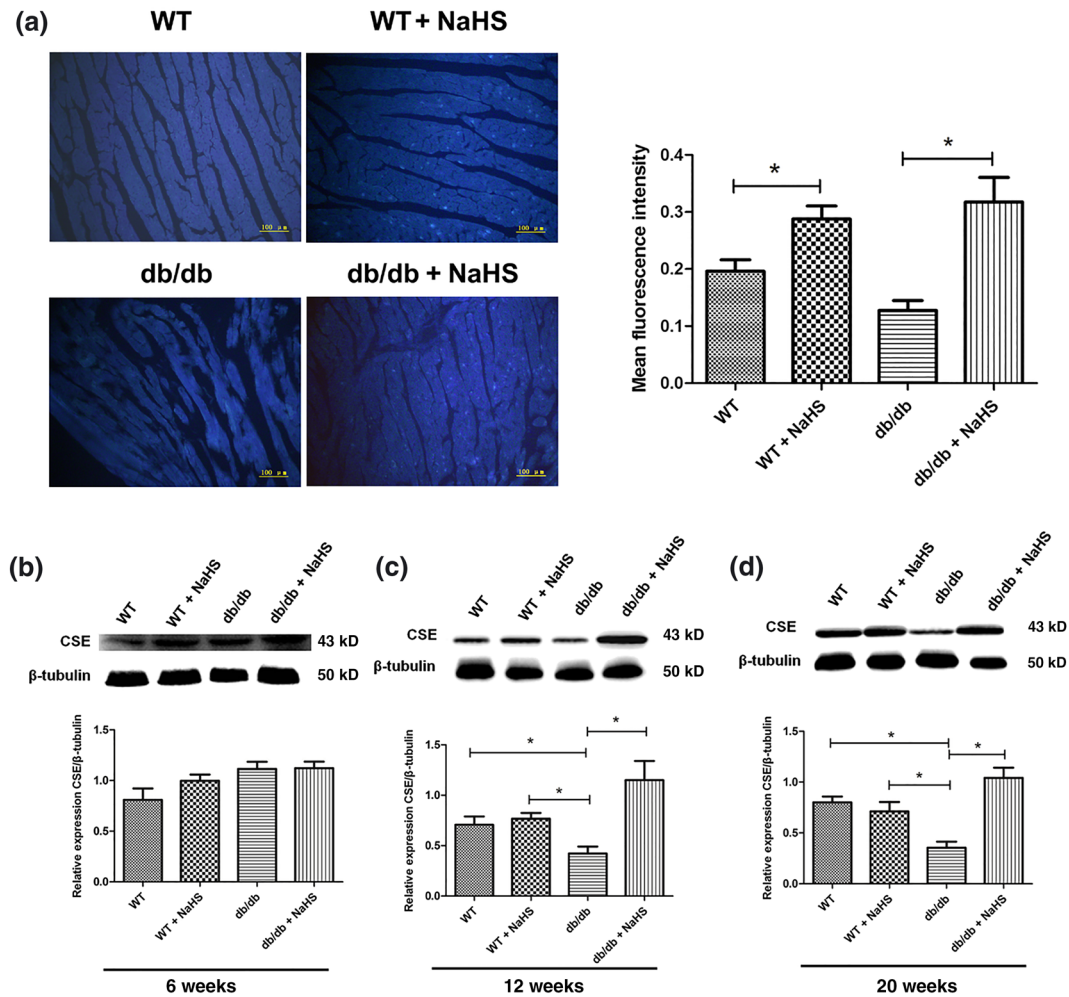


FIGURE 2 H_2S level and CSE expression was decreased in db/db mice. (a) 7-Azido-4-methylcoumarin staining was used to measure H_2S levels in cardiac tissues at 20 weeks, with and without NaHS. (b–d) Quantification of CSE expression in cardiac tissues was carried out by Western blotting at 6, 12, and 20 weeks treated with NaHS, respectively. Data shown are means \pm SD; $n = 6$, * $P < 0.05$, significantly different as indicated; one-way ANOVA

expression of ER stress-associated proteins, p-PERK (Thr⁹⁸¹)/PERK, Bip, ATF4, p-eIF2 α (Ser⁵¹)/eIF2 α , and CHOP. These marker proteins were up-regulated in 12- and 20-week-old db/db mice but exogenous H_2S reversed these alterations (Figure 3a,b). To further study whether H_2S could suppress ER stress in vitro, ER stress-associated proteins were detected in NRCMs. We found that exogenous H_2S also attenuated ER stress in vitro (Figure 3c). NAC (an ROS scavenger) treatment also decreased ER stress effect, like NaHS, indicating the suppression of ER stress by H_2S might be related to its antioxidative effect.

3.4 | Enrichment and clustering analysis of quantitative cardiac structural protein data sets, based on gene ontology annotations

To confirm that the ubiquitination levels of cardiac structural proteins were regulated by NaHS treatment of db/db mice, we analysed the cardiac structural protein proteome data set for four enrichment gene ontology categories: cellular component, molecular function, biological

process, and Kyoto Encyclopedia of Genes and Genomes (KEGG) pathway. The cellular component category (Figure 4a) showed that NaHS treatment had a marked effect on the expression of cardiac structural proteins. Moreover, the enrichment analysis of molecular functions (Figure 4b) showed that proteins involved in the structural constituent of cytoskeleton, muscle, and motor activity were enriched after NaHS treatment. In the biological process category (Figure 4c), proteins related to regulation of muscle system processes, muscle contraction, regulation of heart contraction, tissue morphogenesis, and tissue regeneration were also enriched with NaHS treatment. To identify cellular pathways regulated by NaHS treatment, we performed a pathway clustering analysis of the H_2S -responsive proteome for pathways from the KEGG (Figure 4d). The results showed that hypertrophic cardiomyopathy, dilated cardiomyopathy, and cardiac muscle contraction were the most prominent pathways enriched in quantiles with increased protein level in db/db mice treated by NaHS, suggesting a role of exogenous H_2S in these pathways. In summary, gene ontology enrichment and KEGG pathway-based cluster analysis

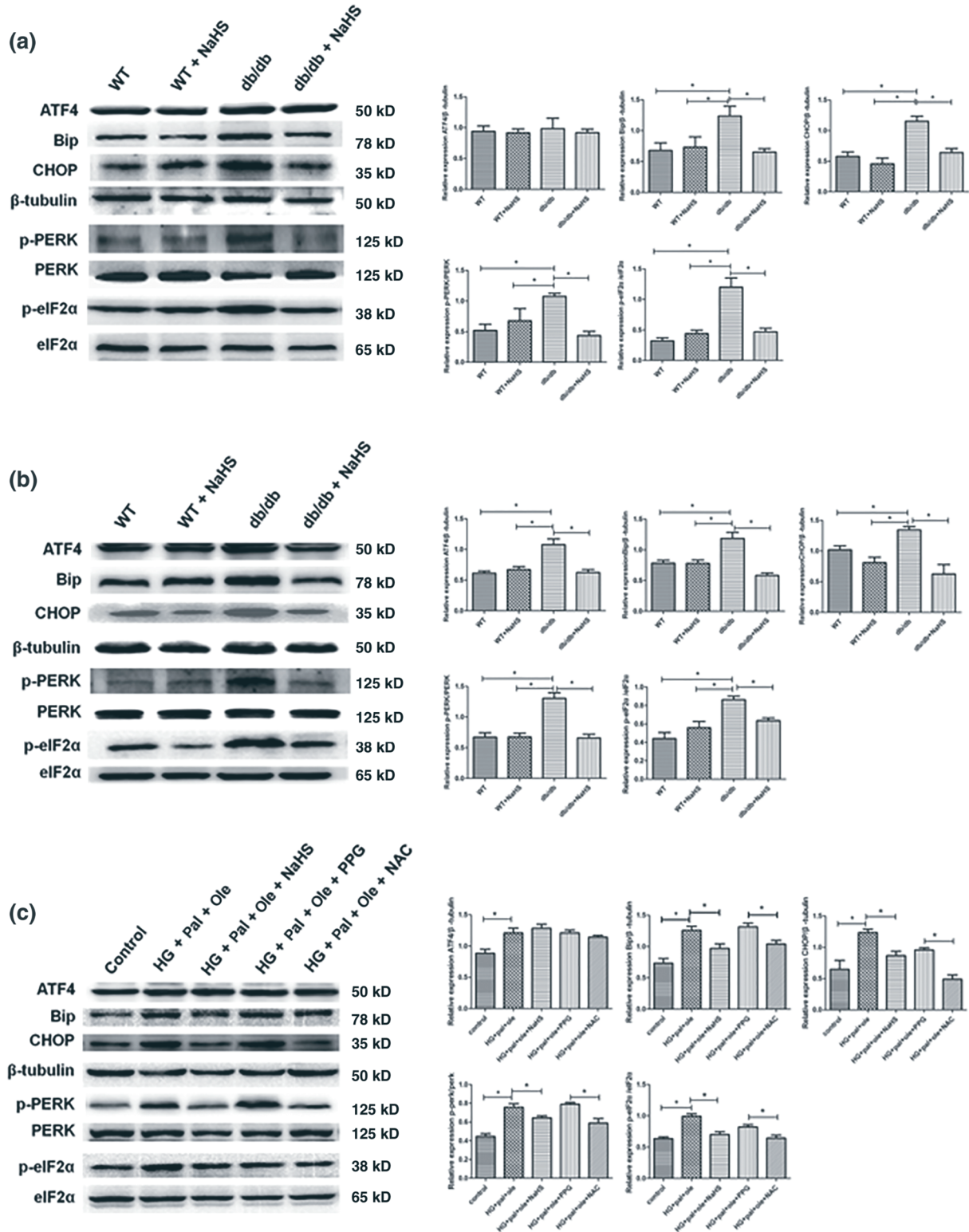
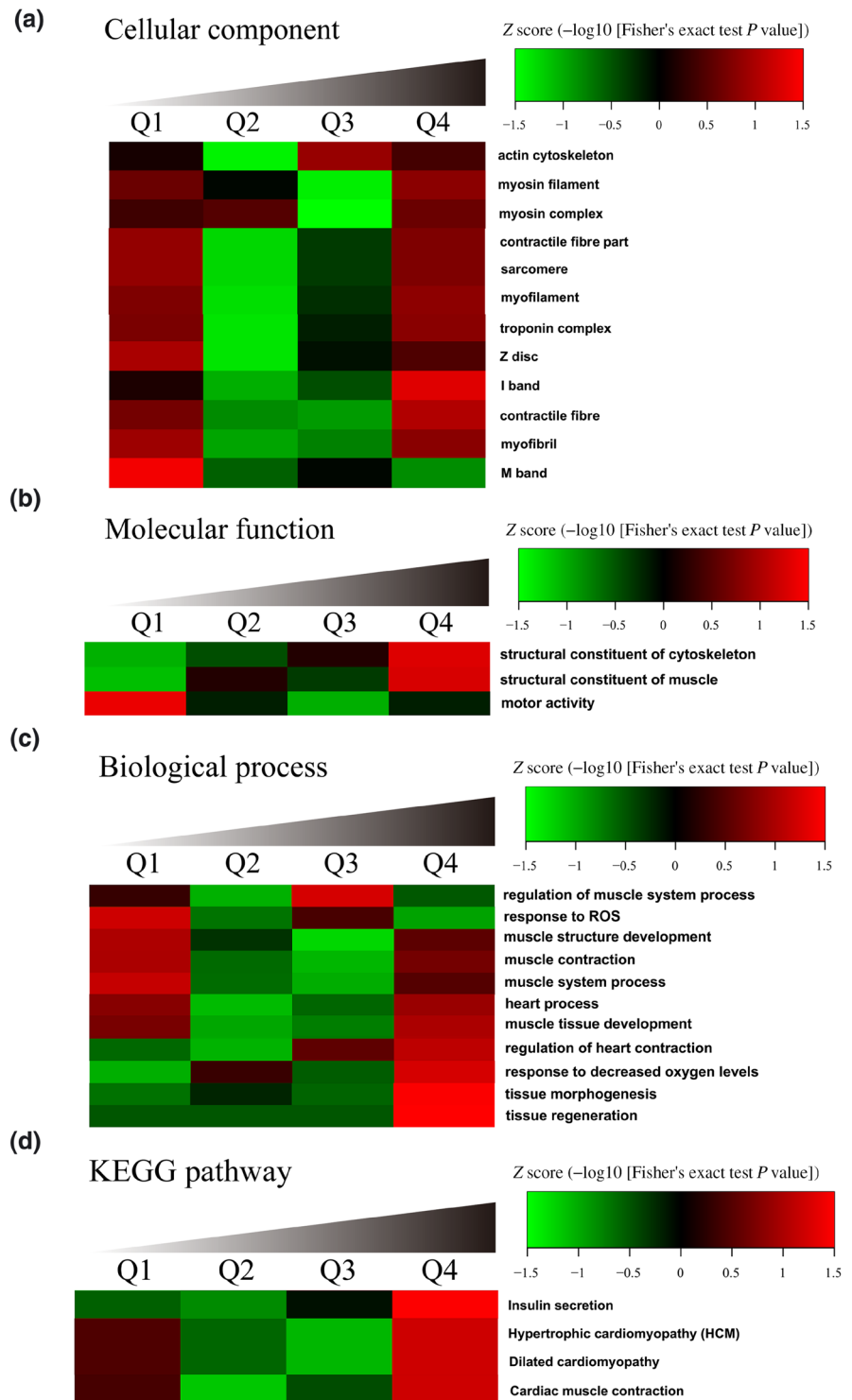


FIGURE 3 Effect of exogenous H_2S on levels of ER stress in vivo and in vitro. (a, b) The expression of protein markers of ER stress, in cardiac tissues, was assessed by Western blotting, in db/db mice at 12 and 20 weeks, treated with NaHS. (c) Western blotting analysis the expression of protein markers of ER stress in NRCMs, incubated with HG (40 mM) + palmitate (Pal, 400 μ M) + oleate (Ole, 100 μ M), HG + Pal + Ole + NaHS (100 μ M), HG + Pal + Ole + PPG (10 nM, an irreversible competitive CSE inhibitor), and HG + Pal + Ole + NAC (100 μ M, an inhibitor of ROS) for 72 hr. Data shown are means \pm SD; $n = 6$, * $P < 0.05$, significantly different as indicated; one-way ANOVA

FIGURE 4 Enrichment and clustering analysis, based on gene ontology annotations, of quantitative data sets of cardiac structural proteins. Using KEGG standard peptides, normalized affinity enrichment followed by label-free quantitative proteomics strategy, quantitative lysine ubiquitylation analysis was performed in a pair of mouse myocardial tissues. Proteins were classified by GO annotation into three categories: biological process, cellular compartment, and molecular function. For each category, we used the Functional Annotation Tool of DAVID Bioinformatics Resources 6.7 to identify enriched GO against the background of *Homo sapiens*. A two-tailed Fisher's exact test was employed to test the enrichment of the protein-containing IPI entries against all IPI proteins. Correction for multiple hypothesis testing was carried out using standard false discovery rate control methods. The GO with a corrected *P*-value <0.05 is considered significant. The quantified Kub proteins in this study were divided, according to the quantification ratio, to generate four quantiles: Q1 (0–15%), Q2 (15–50%), Q3 (50–85%), and Q4 (85–100%). The relative fold change was db/db versus db/db + NaHS. The green colour means *Z* score <0, and this ratio is less than the average. The red colour means *Z* score >0, and this ratio is more than the average. (a) Cellular component, (b) molecular function, (c) biological process, and (d) KEGG pathway analysis were identified by bioinformatic analysis



results showed that the ubiquitination levels of cardiac structural proteins showed many differences in db/db mice from those treated by NaHS based on enrichment.

3.5 | Exogenous H₂S attenuated the degradation of MYH6 and MyL2 in vivo

Our earlier experiments had demonstrated that there was structural damage in the hearts of db/db mice (Figure 1b). Further analysis

showed that the expression of two structural proteins, MYH6 and MyL2, were lower in the cardiac tissues of db/db mice, compared with those of db/db mice treated by NaHS (Figure 5a). The level of ubiquitination induced by ER stress can lead to degradation of cardiac structural proteins (Baskin & Taegtmeier, 2011; Wiersma et al., 2017; Willis, Schisler, Li, et al., 2009; Willis, Schisler, Portbury, & Patterson, 2009). In our study, the ubiquitination level in the hearts of db/db mice was up-regulated in untreated mice, compared with that in db/db mice treated by NaHS (Figure 5b). MuRF1, an E3 ubiquitin

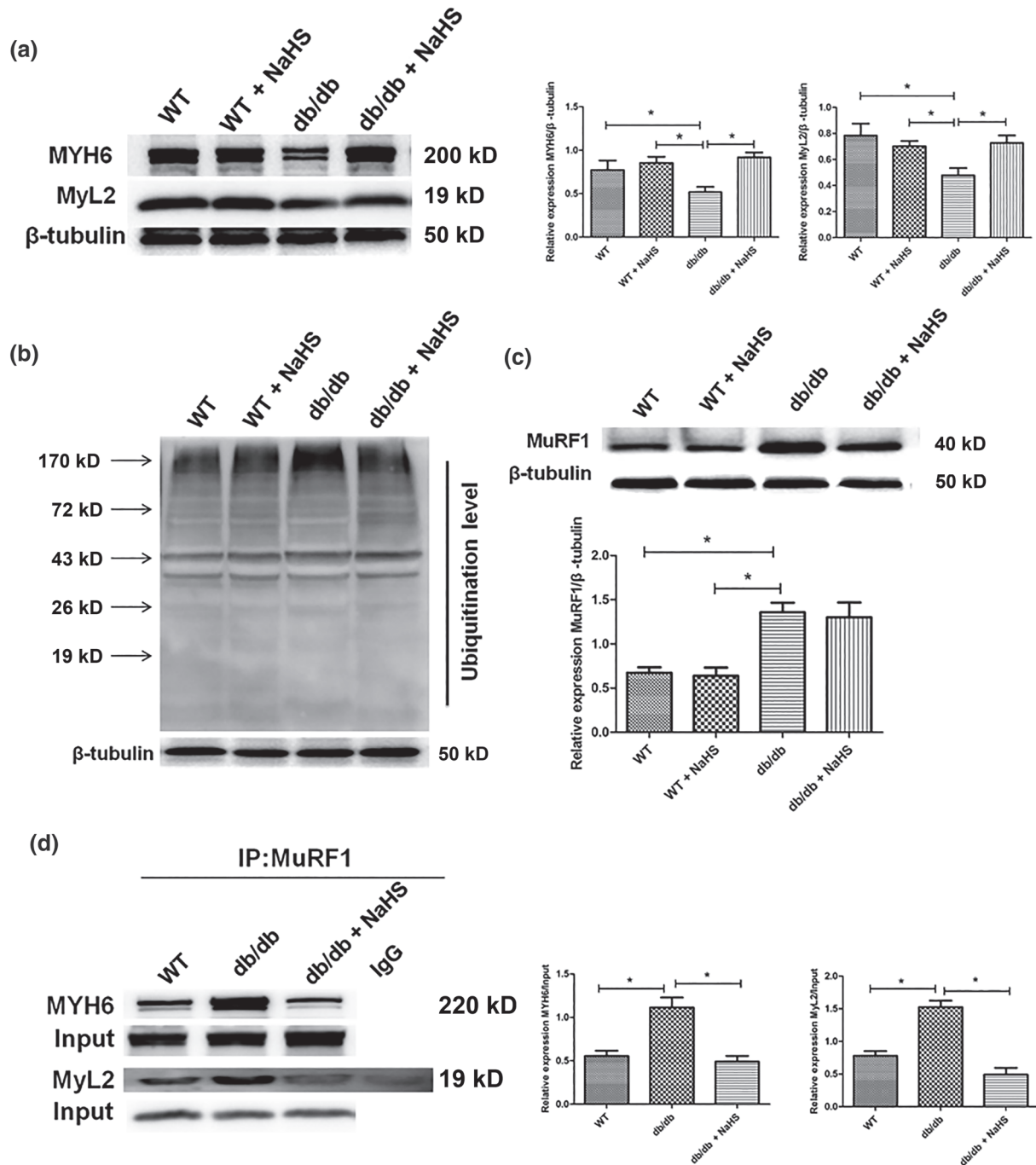


FIGURE 5 Exogenous H_2S protected cardiac structure in *db/db* mice. (a) The expression of cardiac structural proteins MYH6 and MyL2 was measured with Western blotting at 20 weeks treated with NaHS. (b) The ubiquitination level of cardiac tissues was tested by Western blotting. (c) Quantification of MuRF1 expression in cardiac tissues was carried out by Western blotting. (d) Cardiac tissues lysate were immunoprecipitated with anti-MuRF1 antibody and then immunoblotted with antibodies specific for MYH6 and MyL2. Data shown are means \pm SD; $n = 6$, $*P < 0.05$, significantly different as indicated; one-way ANOVA

ligases, is associated with cardiac structure and skeletal muscle degradation (S. N. Chen et al., 2012; Gielen et al., 2012; Kedar et al., 2004; Maejima et al., 2014). Our results revealed that the expression of MuRF1 was increased in the heart of *db/db* mice and that MuRF1 was decreased after treatment with NaHS (Figure 5c). Further

experiments using immunoprecipitation showed that exogenous H_2S weakened the interaction between MuRF1 and MYH6 and MyL2 (Figure 5d). Taken together, the present findings indicate that exogenous H_2S could attenuate the degradation of cardiac structural proteins by MuRF1 in the hearts of *db/db* mice.

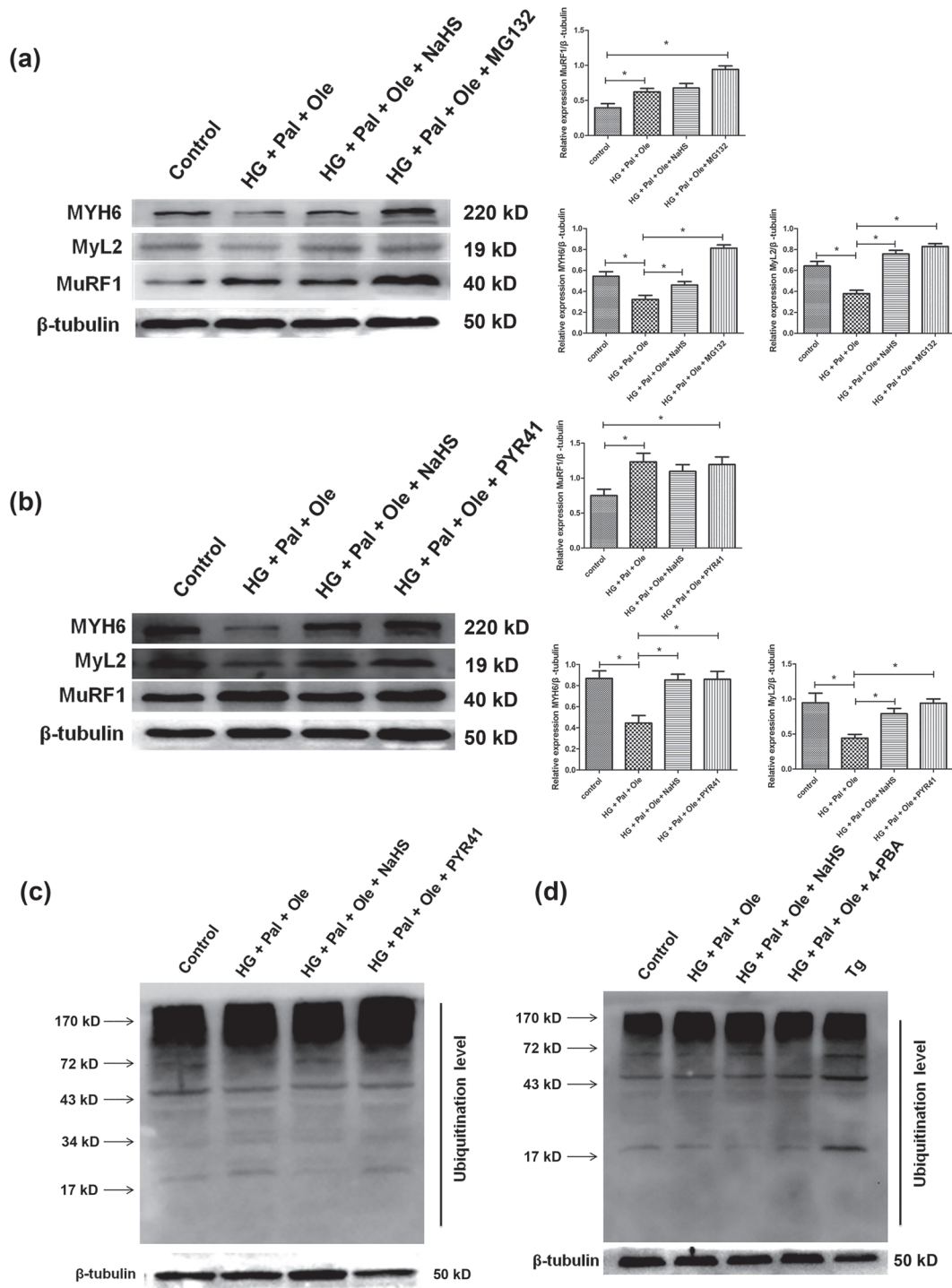


FIGURE 6 Effect of exogenous H_2S on ubiquitination level of cardiac structural proteins in neonatal rat cardiomyocytes. (a, b) NRCMs exposed to HG + Pal + Ole conditions for 72 hr and then treated with MG132 (20 μ M, an inhibitor of proteasome) for 30 min, or PYR41 (3 μ M, an inhibitor of ubiquitin-activating enzyme [E1]), for 2 hr. Expression of MYH6, MyL2, and MuRF1 were measured with Western blotting. (c) The ubiquitination level in NRCMs treated with PYR41, was assessed by Western blotting. (d) The ubiquitination level was assessed by Western blotting in NRCMs under HG + Pal + Ole conditions, with 4-PBA (5 mM, an inhibitor of endoplasmic reticulum stress) and control + thapsigargin (Tg, 100 μ M, an inducer of endoplasmic reticulum stress). Drugs were added directly into the culture for 48 hr. (e) The ubiquitination level in NRCMs was assessed by Western blotting, under conditions of HG (40 mM) + palmitate (Pal, 400 μ M) + oleate (Ole, 100 μ M), HG + Pal + Ole + NaHS (100 μ M), HG + Pal + Ole + PPG (10 nM, an irreversible competitive CSE inhibitor), and HG + Pal + Ole + NAC (100 μ M, an inhibitor of ROS) for 72 hr. (f) NRCMs were immunoprecipitated with anti-MuRF1 antibody and then immunoblotted with antibodies specific for MYH6 and MyL2. Data shown are means \pm SD; $n = 6$, * $P < 0.05$, significantly different as indicated; one-way ANOVA

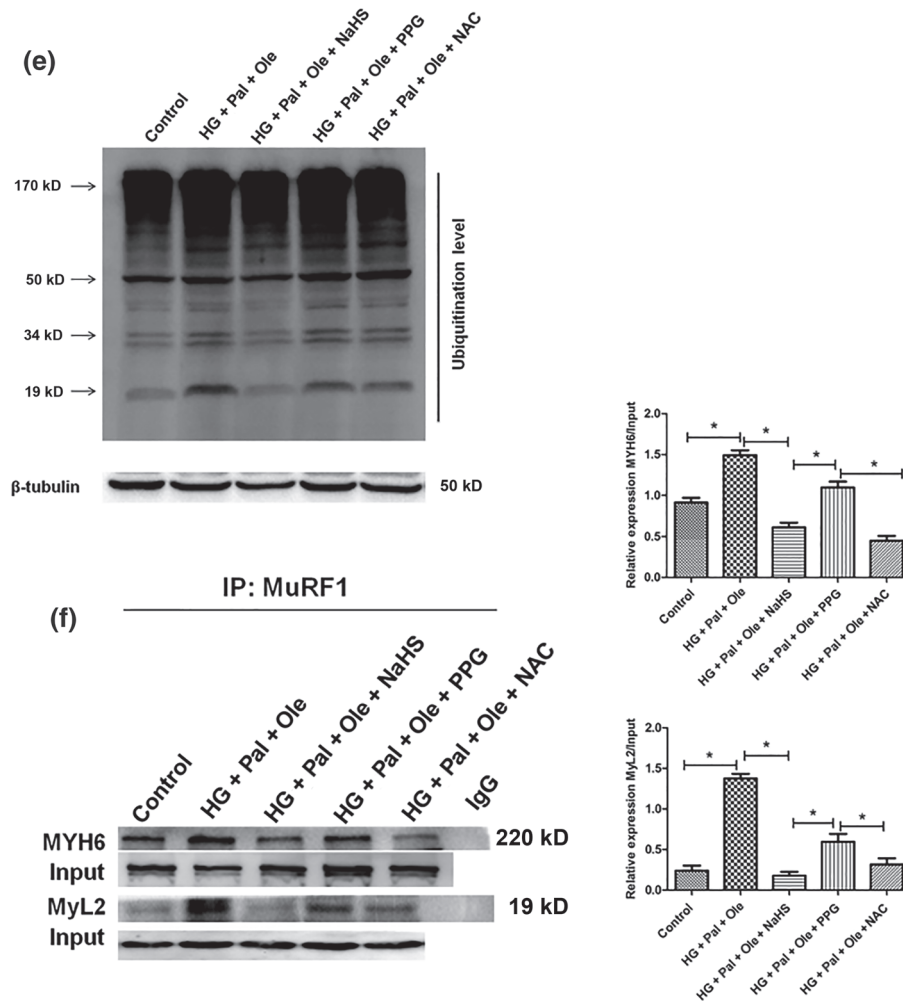


FIGURE 6 Continued.

3.6 | Exogenous H₂S down-regulated the ubiquitination level of cardiac structural proteins by reducing the expression of MuRF1 in vitro

We further investigated whether exogenous H₂S protected cardiac structural proteins through down-regulation of MuRF1. Expression of MuRF1 in NRCMs was increased under the HG + Pal + Ole conditions, and this increased reversed with exogenous H₂S. The protein levels of MYH6 and MyL2 declined under HG + Pal + Ole conditions and were restored by exogenous H₂S. Two different enzyme inhibitors, MG132 (26S proteasome inhibitor, 25 nM) and PYR41 (E1 ubiquitin-activating enzyme inhibitor, 3 μ M) inhibited the degradation of MYH6 and MyL2 in NRCMs (Figure 6a,b). Moreover, the ubiquitination level declined when E1 ubiquitin-activating enzyme was inhibited in NRCMs (Figure 6c). There is evidence that ER stress initiates ubiquitinated degradation (Schlossarek, Frey, & Carrier, 2014; Swatek & Komander, 2016; P. Xu et al., 2009) and we therefore treated NRCMs with thapsigargin (100 μ M, an inducer of ER stress) and 4-PBA (an inhibitor of ER stress) to assess their effects on ubiquitination levels in our model. As expected, ubiquitination levels in NRCMs were raised by thapsigargin, but decreased by 4-PBA

(Figure 6d). Our results also confirmed that the ubiquitination level was decreased in both NaHS and NAC groups. PPG (an irreversible competitive CSE inhibitor) elevated the ubiquitination level (Figure 6e). To analyse how H₂S suppressed ubiquitination, immunoprecipitation was used to measure the interaction between MuRF1 and MYH6 and MyL2 in vitro. The results showed that exogenous H₂S weakened the interaction between MuRF1 and MYH6 and MyL2 whereas PPG improved the interaction between MuRF1 and MYH6 and MyL2. The interaction between MuRF1 and MYH6 and MyL2 was also enhanced by NAC (Figure 6f). Taken together, those findings demonstrate that exogenous H₂S could decrease the expression of MuRF1 and the ubiquitination levels in vitro.

3.7 | MuRF1 siRNA and mutation attenuated the degradation of cardiac structural proteins

To further study the role of MuRF1 in the degradation of cardiac structural proteins, we used MuRF1 siRNA to knock down the expression of MuRF1 in NRCMs, using scramble siRNA as a negative control (Figure 7a). When the expression of MuRF1 was blocked, the protein

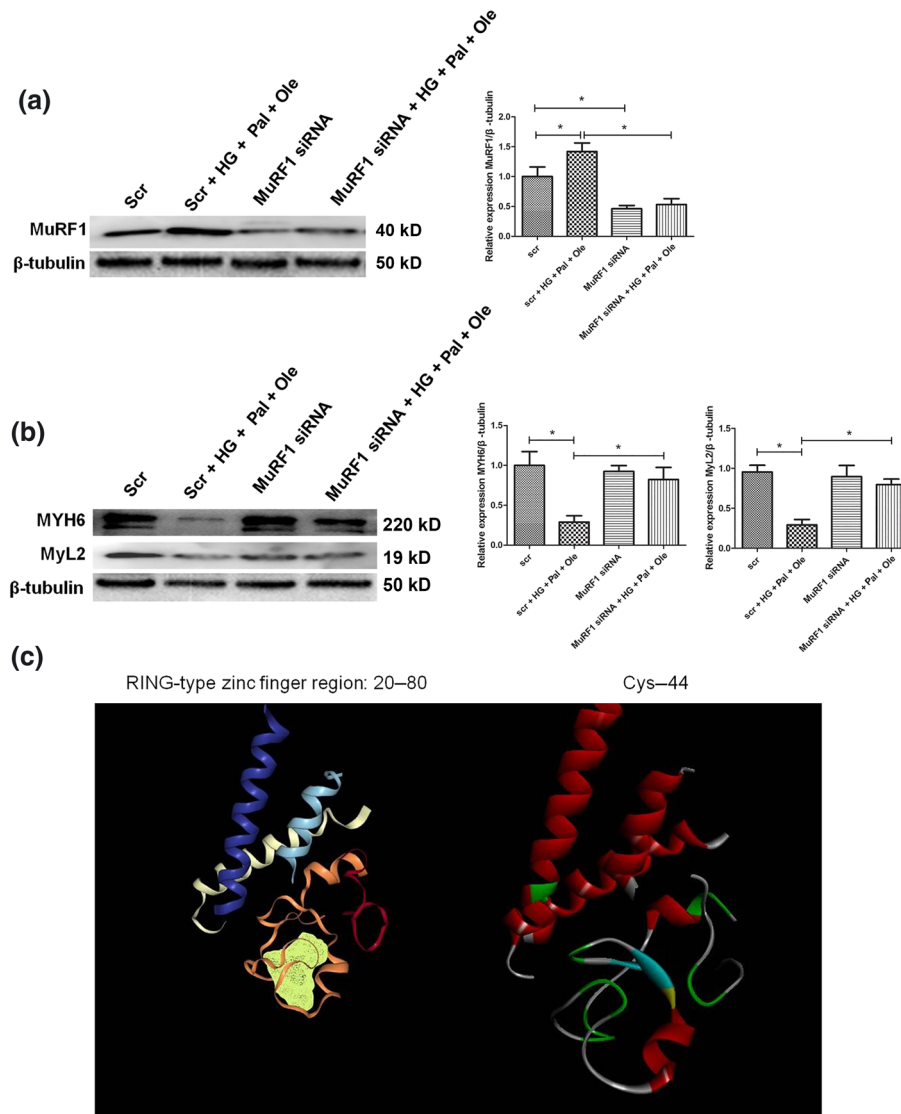


FIGURE 7 Deletion of MuRF1 could attenuate the degradation of cardiac sarcomere. (a, b) After MuRF1 siRNA or scramble siRNA was transfected into NRCMs for 24 hr, the cells were exposed to HG + Pal + Ole conditions for 72 hr. MuRF1, MYH6, and MyL2 protein expressions were measured with Western blotting. (c) The active centre of MuRF1 was predicted by computational method. (d) A mutant MuRF1 (Cys⁴⁴ to alanine) and the vector control were transfected into NRCMs for 12 hr and then exposed to HG + Pal + Ole conditions in the presence or absence of NaHS (100 μ M) for 72 hr. Expression of MYH6, MyL2, and MuRF1 was detected by Western blotting. (e) The ubiquitination level. (f) Extracts of NRCMs were immunoprecipitated with anti-MuRF1 antibody and then immunoblotted with antibodies specific for MYH6 and MyL2. Data shown are means \pm SD; $n = 6$, * $P < 0.05$, significantly different as indicated; one-way ANOVA

level of MYH6 and MyL2 was not reduced (Figure 7b). MuRF1 contains a RING-type zinc finger region, containing 20–80 amino acids. We used bioinformatics methods to analyse and predict the structure of the active site of MuRF1. MuRF1 consists of 350 amino acids and contains 17 cysteine residues, and is involved in ubiquitination through to its RING-type zinc finger domain. The bioinformatics analysis of MuRF1 predicted six active centres. However, only two of active centres had the greatest correlation with cysteine residues. They were the sequences from residues 23 to 79 and from residue 117 to 159 amino acid, and they were exactly RING-type zinc finger domain and B-box-type zinc finger domain. Based on this analysis,

we mutated the Cys⁴⁴ in the RING-type zinc finger domain to alanine. The Cys⁴⁴ plays a crucial role in the activity of MuRF1 (Figure 7c). Mutants of MuRF1 at Cys⁴⁴ were transfected into NRCMs. The expression of MYH6 and MyL2 increased after transfection with the mutant MuRF1, compared with the vector group (Figure 7d). The ubiquitination level declined, as mutant MuRF1 abolished its ubiquitin ligase function (Figure 7e). Immunoprecipitation was used to detect the interaction between MuRF1 and MYH6 and MyL2. The mutant MuRF1 could not interact with MYH6 and MyL2 (Figure 7f). The present studies suggest that MuRF1 plays a pivotal role in the degradation of cardiac structural proteins.

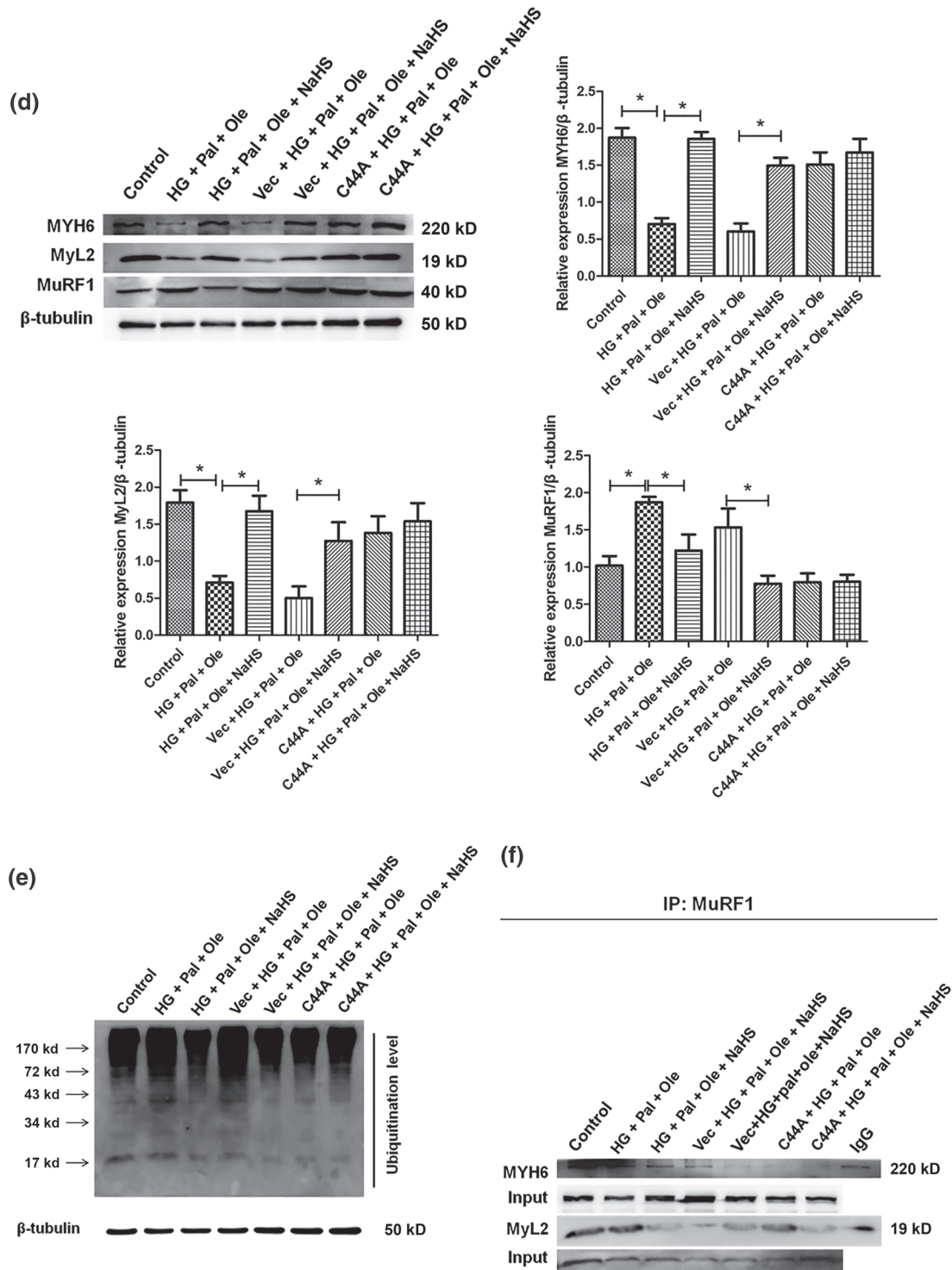


FIGURE 7 Continued.

3.8 | Polysulfidation protected cardiac structural proteins in DCM

Protein polysulfidation plays critical role in post-translational modification by targeting specific cysteine residue(s) which could change local protein structure and activity (Akaike et al., 2017). Polysulfidation could activate sulfhydryl groups, which are believed to mediate

numerous cellular responses initiated by H₂S (Greiner et al., 2013; Shimizu et al., 2017). SSP4, a newly developed fluorescent probe, was used to detect the production of polysulfides in the cardiac tissues of db/db mice. Polysulfides were observed in WT + NaHS and db/db + NaHS groups but not in the WT and db/db groups (Figure 8a). Moreover, biotin-switch assay was also used to detect protein polysulfidation. The results showed that NaHS enhanced

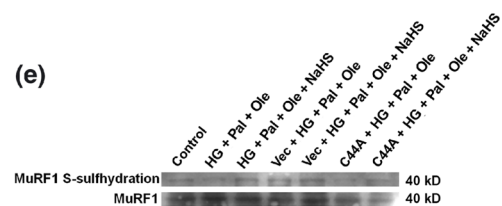
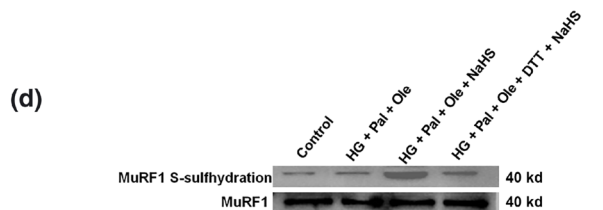
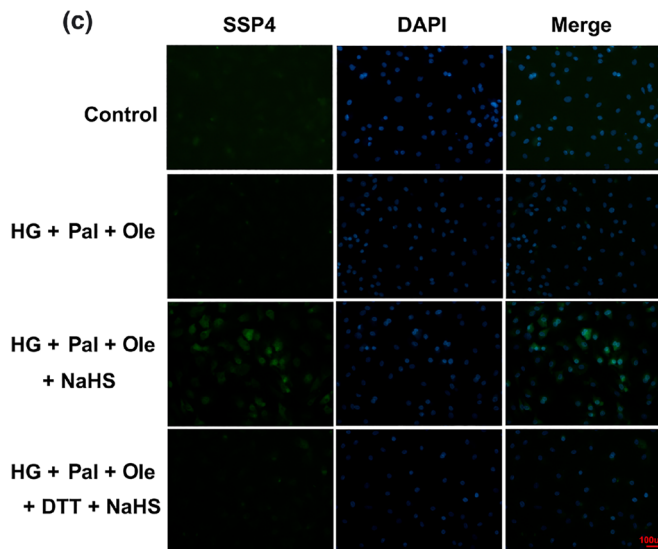
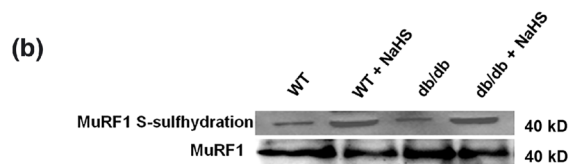
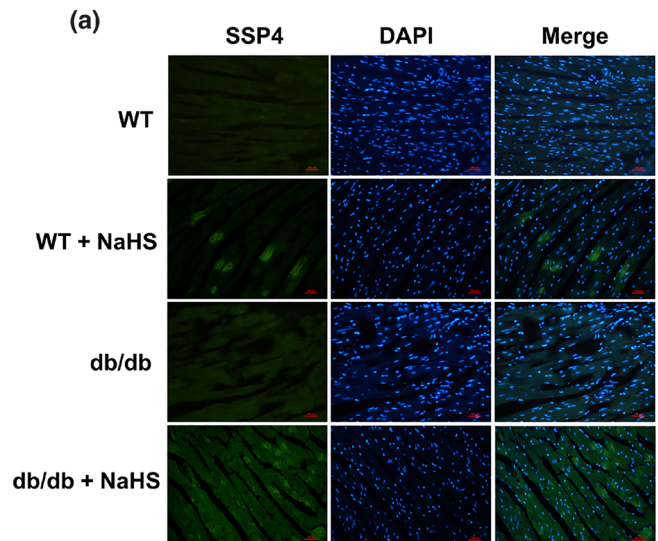


FIGURE 8 Polysulfidation played a crucial role in improvement of DCM in db/db mice. (a) The polysulfidation level was measured with the fluorescent probe, SSP4, in cardiac tissues. Bar = 100 μ m. (b) Quantification of polysulfidation in cardiac tissues was carried out by Western blotting. (c, d) Polysulfidation production in NRCMs was assayed, using the fluorescent probe, SSP4, or by Western blotting. DTT (1 mM, 30 min, an inhibitor of disulfide bonds). Bar = 100 μ m. (e) Polysulfidation production in NRCMs, transfected with MuRF1-Cys⁴⁴ mutant, was assessed by Western blotting. Data shown are means \pm SD; $n = 6$, * $P < 0.05$, significantly different as indicated; one-way ANOVA

polysulfidation formation both in the hearts of WT and db/db mice (Figure 8b). We also identified the effect of H₂S on polysulfide formation in vitro. NaHS elevated polysulfidation levels in NRCMs and DTT (1 mM, an inhibitor of polysulfidate formation, which abolished the effect of NaHS on polysulfidation formation (Figure 8c). The biotinswitch assay also showed that exogenous H₂S promoted polysulfidation formation and DTT abolished the effect of NaHS on polysulfidation formation (Figure 8d). After transfection of NRCMs with the Cys⁴⁴ mutant MuRF1, the polysulfidation of MuRF1 was decreased compared with the vector with NaHS group (Figure 8e). The results indicate that H₂S can promote polysulfidation formation and attenuate the degradation of MYH6 and MyL2.

4 | DISCUSSION

In the present study, we found that (a) H₂S level and CSE protein expression level in the myocardium were decreased in db/db mice; (b) exogenous H₂S reversed ER stress, including impairment of the function of cardiomyocytes and structural damage in db/db mice; (c) exogenous H₂S could suppress MYH6 and MyL2 ubiquitination level in cardiac tissues of db/db mice; and (d) MuRF1 was modified by S-sulfhydration following treatment with exogenous H₂S to reduce the interaction between MuRF1 and MYH6 and MyL2. These data suggested that an impaired H₂S/CSE system contributed to cardiac structural damage. Moreover, our results revealed the possibility that

H₂S supplementation might be a significant therapeutic approach to attenuate cardiac damage in diabetic patients.

In diabetic hearts, cardiomyocytes have to increase fatty acid oxidation to maintain ATP production, which is accompanied by increased ROS production, which has adverse effects on cell functions (Pulinilkunnil & Rodrigues, 2006). ROS may damage DNA, proteins, and membrane lipids, leading to significant apoptosis, fibrosis, and heart failure with preserved EF, similar to restrictive cardiomyopathy (Zhang, Perino, Ghigo, Hirsch, & Shah, 2013). This condition subsequently evolves into heart failure with reduced EF, resembling dilated cardiomyopathy. In our study, we found that EF (%) and FS (%) were decreased, the Z-line was ruptured with a degraded M-line, and the sarcoplasmic reticulum (SR) was significantly swollen in 20-week-old db/db mice. Therefore, db/db mice were considered to be exhibiting cardiomyopathy at 20 weeks.

Hyperglycaemia and hyperlipidaemia enhance oxidative stress, and ROS accumulation may promote protein misfolding and aggregation in the ER, which is called ER stress, and contributes to the aetiology and pathogenesis of Type 2 diabetes. ER protein misfolding activates the unfolded protein response (UPR), a conserved signalling system that initiates many processes to restore proteostasis (Calamai, Chiti, & Dobson, 2005). Our present study demonstrates that hyperglycaemia and hyperlipidaemia induce ER stress in cardiac muscle, contributing to cardiac dysfunctions. Three markers of ER stress (Bip, p-eIF2 α , and p-PERK) were markedly increased in db/db mice. When the UPR fails to resolve ER stress, maladaptive features of the UPR, called maladaptive stress, are responsible for the tissue damage and organ

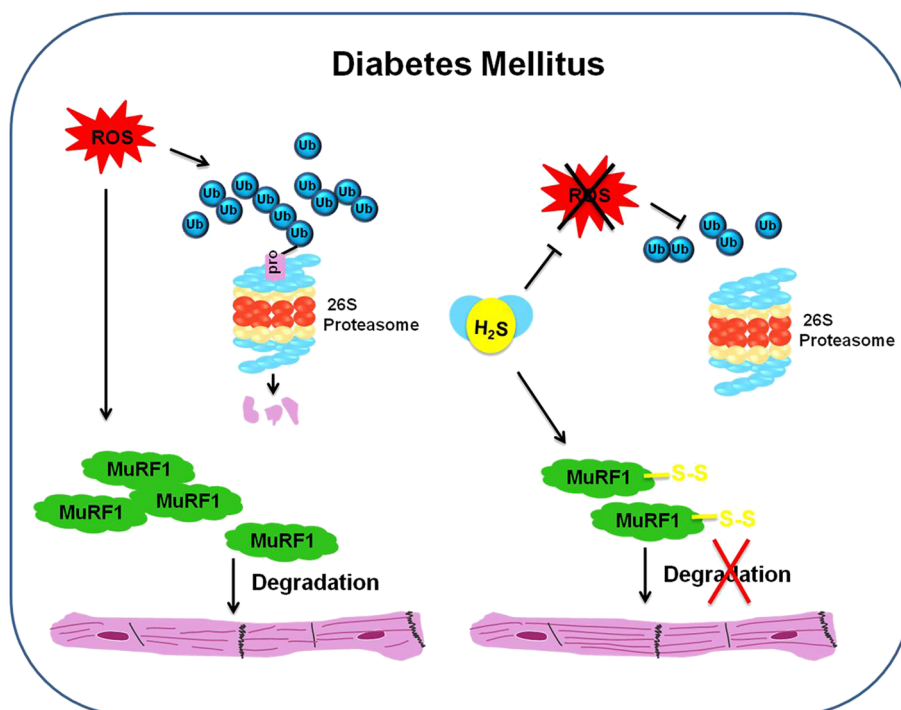


FIGURE 9 The role of H₂S in regulation of the degradation of cardiac structural proteins in a model of Type 2 diabetes. In Type 2 diabetes, increasing amounts of ROS promote ubiquitination and MuRF1 expression, which then lead to cardiac sarcomere degradation. H₂S decreases ubiquitination levels and MuRF1 expression. Also, H₂S can modulate the S-sulfhydration on MuRF1 to decrease its activity and thus to protect cardiac structural proteins

dysfunction (C. Xu, Bailly-Maitre, & Reed, 2005). Bip, as a molecular chaperone, regulates the unfolded proteins. PERK and eIF2 α constitute the core stress regulator of UPR and transduce signals from ER to the cytosol and nucleus during ER stress (Ron & Walter, 2007). CHOP, which is a transcription factor, decreases Bcl-2 transcription and induces apoptosis. As our present results have shown, ER stress was induced in db/db mice and in NRCMs exposed to HG + Pal + Ole conditions. However, levels of ER stress can be attenuated by NaHS and NAC, the antioxidant and ROS scavenger. The misfolded proteins are damaged by ER-associated degradation (Calamai et al., 2005). ER-associated degradation is a four-step quality control process for removing misfolded proteins from the ER by the cytosolic ubiquitin-proteasome system (Olzmann, Kopito, & Christianson, 2013). Ubiquitin is attached to a substrate lysine, through an enzymic cascade, which includes an ubiquitin-activating enzyme (E1), an ubiquitin-conjugating enzyme (E2), and an ubiquitin-protein ligase (E3; C. Chen et al., 2014). E1 is the first step in ubiquitination. PYR41 is a low MW inhibitor of E1 ubiquitin-activating enzyme, which suppresses the subsequent ubiquitination reaction. In our study, when NRCMs were treated with PYR41 under HG + Pal + Ole conditions; the ubiquitination of cardiomyocyte proteins was suppressed. E3 ubiquitin ligases target them for degradation by cytosolic proteasomes. The MuRF family consists of RING finger E3 ubiquitin ligases expressed specifically in cardiac and skeletal muscles. MuRF1 levels are decreased in denervation-induced skeletal muscle atrophy, and MuRF1 is located in the M-line region and colocalizes with α -actinin, one of the major components of the Z-disc in heart tissues (Vidal & Hetz, 2012). In addition, MuRF1 regulates microtubule dynamics, myofibril structure, and muscle metabolism, including carbohydrate metabolism (Bogomolovas, Gasch, & Simkovic, 2014; Hirner et al., 2008; Perera, Holt, Mankoo, & Gautel, 2011). In this study, we found that increased expression and activity of the ubiquitin proteasome proteolytic pathway, that is, a marked up-regulation of MuRF1, play essential roles in muscle rupture in DCM. Using LC-MS/MS protein analysis, we identified 147 proteins that were hyper-ubiquitinated in the heart of db/db mice, compared to those after treatment with NaHS, and six proteins belong to cardiac muscle structural proteins (Table S4). The ubiquitination levels of two cardiac muscle structural proteins MYH6 and MyL2, after treatment with NaHS were clearly lower than those in the hearts of untreated db/db mice. The ubiquitin-26S proteasome system, as a cellular house-keeping system, degrades the selected target proteins by the 26S proteasome (Marshall, Li, Gemperline, Book, & Vierstra, 2015), which is a 2.5-MDa, self-compartmentalized proteolytic machine located in the cytosol (Finley, 2009). It includes two distinct subunits, the 20S core protease and the 19S regulatory particle (Bhattacharyya, Yu, Mim, & Matouschek, 2014) and it plays a central important role in the ubiquitin-26S proteasome system. In this study, MG132, a proteasome inhibitor, decreased the degradation of MYH6 and MyL2 in NRCMs HG + Pal + Ole conditions.

H₂S, as a novel gasotransmitter, exerts a range of physiological and pathophysiological effects, particularly in the cardiovascular system (Nagpure & Bian, 2016; Wallace & Wang, 2015). Accumulating evidence suggests that production of endogenous H₂S or the

administration of exogenous H₂S can attenuate myocardial injury after ischaemia or reperfusion and decrease BP and resist oxidative stress (X. Chen et al., 2017; L. Li et al., 2008; D. Wu et al., 2015). In our study, we noticed that the expression of CSE, a key enzyme to produce H₂S in cardiovascular system, was reduced in db/db mice (Figure 2c,d). Immunoprecipitation was carried out to detect the interaction between CSE and ubiquitin, we found that CSE was modified by ubiquitin and degraded by the ubiquitin-proteasome system. After treatment with NaHS, the ubiquitination of CSE was decreased (Figure S3). H₂S acts as a secondary messenger, by directly modulating the function of downstream targets (Mustafa et al., 2009). PPG is a specific inhibitor of CSE and thus inhibited endogenous H₂S production and increased ER stress and ubiquitination. H₂S also covalently modifies cysteine residues on target proteins in a process known as S-sulfhydration (Meng et al., 2016; Paul & Snyder, 2012; Paul & Snyder, 2015). In this instance, sulfur derived from H₂S binds to the thiol group of a target cysteine residue to form a hydropersulfide moiety (-SSH; Lu, Kavalier, Lukyanov, & Gross, 2013; Pennick, Poole, Dennis, & Smyth, 2012). We found that NaHS increased the S-sulfhydration in MuRF1 (Figure 8) but that DTT, a blocker of S-sulfhydration, decreased MuRF1 S-sulfhydration. In addition, NaHS regulated MuRF1 activity and inhibited the interaction of MuRF1 with MYH6 or MyL2. After MuRF1 was mutated at Cys⁴⁴, the S-sulfhydration level of MuRF1 was decreased, and the interaction between MuRF1 and MYH6 and MyL2 was inhibited.

In conclusion, this study has provided evidence that H₂S increased MuRF1 S-sulfhydration at Cys⁴⁴ to regulate MYH6 and MyL2 ubiquitination, thereby preventing cardiac muscle degradation in our model of DCM in db/db mice (Figure 9). H₂S may be a useful therapeutic strategy in DCM in the future.

ACKNOWLEDGEMENT

This work was supported by the National Natural Science Foundation of China (81570340 and 81670344).

AUTHOR CONTRIBUTIONS

X.S., D.Z., F.L., F.L., and W.Z. participated in the research design. X.S., S.P., M.Y., and Y.S. conducted the experiments. X.S., Y.S., H.D., J.C., and B.W. performed the data analysis. X.S., N.L., S.D., and W.Z. wrote the manuscript. All authors reviewed and revised the final version of manuscript and approved manuscript submission.

CONFLICT OF INTEREST

The authors declare no conflicts of interest.

DECLARATION OF TRANSPARENCY AND SCIENTIFIC RIGOUR

This Declaration acknowledges that this paper adheres to the principles for transparent reporting and scientific rigour of preclinical research as stated in the *BJP* guidelines for [Design & Analysis](#), [Immunoblotting and Immunocytochemistry](#), and [Animal Experimentation](#), and as

recommended by funding agencies, publishers, and other organisations engaged with supporting research.

ORCID

Xiaojiao Sun  <https://orcid.org/0000-0002-4165-5260>

REFERENCES

- Akaike, T., Ida, T., Wei, F.-Y., Nishida, M., Kumagai, Y., Alam, M. M., ... Motohashi, H. (2017). CysteinyI-tRNA synthetase governs cysteine polysulfidation and mitochondrial bioenergetics. *Nature Communications*, 8, 1177. <https://doi.org/10.1038/s41467-017-01311-y>
- Alexander, S. P. H., Fabbro, D., Kelly, E., Marrion, N. V., Peters, J. A., Faccenda, E., ... CGTP Collaborators. (2017). The Concise Guide to PHARMACOLOGY 2017/18: Enzymes. *British Journal of Pharmacology*, 174, S272–S359. <https://doi.org/10.1111/bph.13877>
- Baskin, K. K., & Taegtmeyer, H. (2011). AMP-activated protein kinase regulates E3 ligases in rodent heart. *Circulation Research*, 109, 1153–1161. <https://doi.org/10.1161/CIRCRESAHA.111.252742>
- Bhattacharyya, S., Yu, H., Mim, C., & Matouschek, A. (2014). Regulated protein turnover: Snapshots of the proteasome in action. *Nature Reviews. Molecular Cell Biology*, 15, 122–133. <https://doi.org/10.1038/nrm3741>
- Bodine, S. C., Latres, E., Baumhueter, S., Lai, V. K., Nunez, L., Clarke, B. A., ... Glass, D. J. (2001). Identification of ubiquitin ligases required for skeletal muscle atrophy. *Science*, 294, 1704–1708. <https://doi.org/10.1126/science.1065874>
- Bogomolovas, J., Gasch, A., & Simkovic, F. (2014). Titin kinase is an inactive pseudokinase scaffold that supports MuRF1 recruitment to the sarcomeric M-line. 4: 140041.
- Calamai, M., Chiti, F., & Dobson, C. M. (2005). Amyloid fibril formation can proceed from different conformations of a partially unfolded protein. *Biophysical Journal*, 89, 4201–4210. <https://doi.org/10.1529/biophysj.105.068726>
- Calvert, J. W., Coetzee, W. A., & Lefer, D. J. (2010). Novel insights into hydrogen sulfide-mediated cytoprotection. *Antioxidants & Redox Signaling*, 12, 1203–1217. <https://doi.org/10.1089/ars.2009.2882>
- Centner, T., Yano, J., Kimura, E., McElhinny, A. S., Pelin, K., Witt, C. C., ... Labeit, S. (2001). Identification of muscle specific ring finger proteins as potential regulators of the titin kinase domain. *Journal of Molecular Biology*, 306, 717–726. <https://doi.org/10.1006/jmbi.2001.4448>
- Chen, B., Li, W., Lv, C., Zhao, M., Jin, H., Jin, H., ... Tang, X. (2013). Fluorescent probe for highly selective and sensitive detection of hydrogen sulfide in living cells and cardiac tissues. *Analyst*, 138, 946–951. <https://doi.org/10.1039/C2AN36113B>
- Chen, C., Meng, Y., Wang, L., Wang, H. X., Tian, C., Pang, G. D., ... du, J. (2014). Ubiquitin-activating enzyme E1 inhibitor PYR41 attenuates angiotensin II-induced activation of dendritic cells via the IκBα/NF-κB and MKP1/ERK/STAT1 pathways. *Immunology*, 142, 307–319. <https://doi.org/10.1111/imm.12255>
- Chen, S. N., Czernuszewicz, G., Tan, Y., Lombardi, R., Jin, J., Willerson, J. T., & Marian, A. J. (2012). Human molecular genetic and functional studies identify TRIM63, encoding muscle RING finger protein 1, as a novel gene for human hypertrophic cardiomyopathy. *Circulation Research*, 111, 907–919. <https://doi.org/10.1161/CIRCRESAHA.112.270207>
- Chen, X., Zhao, X., Cai, H., Sun, H., Hu, Y., Huang, X., ... Kong, W. (2017). The role of sodium hydrosulfide in attenuating the aging process via PI3K/AKT and CaMKKβ/AMPK pathways. *Redox Biology*, 12, 987–1003. <https://doi.org/10.1016/j.redox.2017.04.031>
- Danaei, G., Finucane, M. M., Lu, Y., Singh, G. M., Cowan, M. J., Paciorek, C. J., ... Ezzati, M. (2011). National, regional, and global trends in fasting plasma glucose and diabetes prevalence since 1980: Systematic analysis of health examination surveys and epidemiological studies with 370 country-years and 2.7 million participants. *Lancet*, 378, 31–40. [https://doi.org/10.1016/S0140-6736\(11\)60679-X](https://doi.org/10.1016/S0140-6736(11)60679-X)
- Finley, D. (2009). Recognition and processing of ubiquitin-protein conjugates by the proteasome. *Annual Review of Biochemistry*, 78, 477–513. <https://doi.org/10.1146/annurev.biochem.78.081507.101607>
- From, A. M., Leibson, C. L., Bursi, F., Redfield, M. M., Weston, S. A., Jacobsen, S. J., ... Roger, V. L. (2006). Diabetes in heart failure: Prevalence and impact on outcome in the population. *The American Journal of Medicine*, 119, 591–599. <https://doi.org/10.1016/j.amjmed.2006.05.024>
- Fu, M., Zhang, W., Wu, L., Yang, G., Li, H., & Wang, R. (2012). Hydrogen sulfide (H₂S) metabolism in mitochondria and its regulatory role in energy production. *Proceedings of the National Academy of Sciences of the United States of America*, 109, 2943–2948. <https://doi.org/10.1073/pnas.1115634109>
- Gielen, S., Sandri, M., Kozarek, I., Kratzsch, J., Teupser, D., Thiery, J., ... Adams, V. (2012). Exercise training attenuates MuRF-1 expression in the skeletal muscle of patients with chronic heart failure independent of age: The randomized Leipzig Exercise Intervention in Chronic Heart Failure and Aging catabolism study. *Circulation*, 125, 2716–2727. <https://doi.org/10.1161/CIRCULATIONAHA.111.047381>
- Greiner, R., Palinkas, Z., Basell, K., Becher, D., Antelmann, H., Nagy, P., & Dick, T. P. (2013). Polysulfides link H₂S to protein thiol oxidation. *Antioxidants & Redox Signaling*, 19, 1749–1765. <https://doi.org/10.1089/ars.2012.5041>
- Harding, S. D., Sharman, J. L., Faccenda, E., Southan, C., Pawson, A. J., Ireland, S., ... NC-IUPHAR. (2018). The IUPHAR/BPS Guide to PHARMACOLOGY in 2018: Updates and expansion to encompass the new guide to IMMUNOPHARMACOLOGY. *Nucleic Acids Research*, 46, D1091–D1106. <https://doi.org/10.1093/nar/gkx1121>
- Hirner, S., Krohne, C., Schuster, A., Hoffmann, S., Witt, S., Erber, R., ... Labeit, D. (2008). MuRF1-dependent regulation of systemic carbohydrate metabolism as revealed from transgenic mouse studies. *Journal of Molecular Biology*, 379, 666–677. <https://doi.org/10.1016/j.jmb.2008.03.049>
- Kedar, V., McDonough, H., Arya, R., Li, H. H., Rockman, H. A., & Patterson, C. (2004). Muscle-specific RING finger 1 is a bona fide ubiquitin ligase that degrades cardiac troponin I. *Proceedings of the National Academy of Sciences of the United States of America*, 101, 18135–18140. <https://doi.org/10.1073/pnas.0404341102>
- Kilkenny, C., Browne, W., Cuthill, I. C., Emerson, M., & Altman, D. G. (2010). Animal research: Reporting in vivo experiments: the ARRIVE guidelines. *British Journal of Pharmacology*, 160, 1577–1579.
- Kimura, Y., Toyofuku, Y., Koike, S., Shibuya, N., Nagahara, N., Lefer, D., ... Kimura, H. (2015). Identification of H₂S₃ and H₂S produced by 3-mercaptopyruvate sulfurtransferase in the brain. *Scientific Reports*, 5, 14774. <https://doi.org/10.1038/srep14774>
- Li, L., Whiteman, M., Guan, Y. Y., Neo, K. L., Cheng, Y., Lee, S. W., ... Moore, P. K. (2008). Characterization of a novel, water-soluble hydrogen sulfide-releasing molecule (GYY4137): New insights into the biology of hydrogen sulfide. *Circulation*, 117, 2351–2360. <https://doi.org/10.1161/CIRCULATIONAHA.107.753467>
- Li, S., Zhang, L., Ni, R., Cao, T., Zheng, D., Xiong, S., ... Peng, T. (2016). Disruption of calpain reduces lipotoxicity-induced cardiac injury by preventing endoplasmic reticulum stress. *Biochimica et Biophysica Acta*, 1862, 2023–2033. <https://doi.org/10.1016/j.bbadis.2016.08.005>

- Lu, C., Kavalier, A., Lukyanov, E., & Gross, S. S. (2013). S-sulfhydration/desulfhydration and S-nitrosylation/denitrosylation: A common paradigm for gasotransmitter signaling by H₂S and NO. *Methods*, *62*, 177–181. <https://doi.org/10.1016/j.ymeth.2013.05.020>
- Maejima, Y., Usui, S., Zhai, P., Takamura, M., Kaneko, S., Zablocki, D., ... Sadoshima, J. (2014). Muscle-specific RING finger 1 negatively regulates pathological cardiac hypertrophy through downregulation of calcineurin A. *Circulation. Heart Failure*, *7*, 479–490. <https://doi.org/10.1161/CIRCHEARTFAILURE.113.000713>
- Marshall, R. S., Li, F., Gemperline, D. C., Book, A. J., & Vierstra, R. D. (2015). Autophagic degradation of the 26S proteasome is mediated by the dual ATG8/ubiquitin receptor RPN10 in Arabidopsis. *Molecular Cell*, *58*, 1053–1066. <https://doi.org/10.1016/j.molcel.2015.04.023>
- Meng, G., Xiao, Y., Ma, Y., Tang, X., Xie, L., Liu, J., ... Ji, Y. (2016). Hydrogen sulfide regulates Krüppel-like factor 5 transcription activity via specificity protein 1 S-sulfhydration at Cys664 to prevent myocardial hypertrophy. *Journal of the American Heart Association*, *5*. <https://doi.org/10.1161/JAHA.116.004160>
- Meng, G., Zhao, S., Xie, L., Han, Y., & Ji, Y. (2018). Protein S-sulfhydration by hydrogen sulfide in cardiovascular system. *British Journal of Pharmacology*, *175*, 1146–1156.
- Mustafa, A. K., Gadalla, M. M., Sen, N., Kim, S., Mu, W., Gazi, S. K., ... Snyder, S. H. (2009). H₂S signals through protein S-sulfhydration. *Science Signaling*, *2*, ra72.
- Nagpure, B. V., & Bian, J. S. (2016). Interaction of hydrogen sulfide with nitric oxide in the cardiovascular system. *Oxidative Medicine and Cellular Longevity* *2016*, 2016, 6904327. <https://doi.org/10.1155/2016/6904327>
- Ni, R., Cao, T., Xiong, S., Ma, J., Fan, G. C., Laceyfield, J. C., ... Peng, T. (2016). Therapeutic inhibition of mitochondrial reactive oxygen species with mito-TEMPO reduces diabetic cardiomyopathy. *Free Radical Biology & Medicine*, *90*, 12–23. <https://doi.org/10.1016/j.freeradbiomed.2015.11.013>
- Olzmann, J. A., Kopito, R. R., & Christianson, J. C. (2013). The mammalian endoplasmic reticulum-associated degradation system. *Cold Spring Harbor Perspectives in Biology*, *5*, a013185. <https://doi.org/10.1101/cshperspect.a013185>
- Pang, G. F., Fan, C. L., Cao, Y. Z., Yan, F., Li, Y., Kang, J., ... Chang, Q. Y. (2015). High throughput analytical techniques for the determination and confirmation of residues of 653 multiclass pesticides and chemical pollutants in tea by GC/MS, GC/MS/MS, and LC/MS/MS: Collaborative study, first action 2014.09. *Journal of AOAC International*, *98*, 1428–1454. <https://doi.org/10.5740/jaoacint.15021>
- Papaoannou, V. E., & Fox, J. G. (1993). Efficacy of tribromoethanol anesthesia in mice. *Laboratory Animal Science*, *43*, 189–192.
- Paul, B. D., & Snyder, S. H. (2012). H₂S signalling through protein sulfhydration and beyond. *Nature Reviews. Molecular Cell Biology*, *13*, 499–507. <https://doi.org/10.1038/nrm3391>
- Paul, B. D., & Snyder, S. H. (2015). H₂S: A novel gasotransmitter that signals by sulfhydration. *Trends in Biochemical Sciences*, *40*, 687–700. <https://doi.org/10.1016/j.tibs.2015.08.007>
- Pennick, M., Poole, L., Dennis, K., & Smyth, M. (2012). Lanthanum carbonate reduces urine phosphorus excretion: Evidence of high-capacity phosphate binding. *Renal Failure*, *34*, 263–270. <https://doi.org/10.3109/0886022X.2011.649657>
- Perera, S., Holt, M. R., Mankoo, B. S., & Gautel, M. (2011). Developmental regulation of MURF ubiquitin ligases and autophagy proteins nbr1, p62/SQSTM1 and LC3 during cardiac myofibril assembly and turnover. *Developmental Biology*, *351*, 46–61. <https://doi.org/10.1016/j.ydbio.2010.12.024>
- Popov, D. (2013). An outlook on vascular hydrogen sulphide effects, signaling, and therapeutic potential. *Archives of Physiology and Biochemistry*, *119*, 189–194. <https://doi.org/10.3109/13813455.2013.803578>
- Pulinilkunnil, T., & Rodrigues, B. (2006). Cardiac lipoprotein lipase: Metabolic basis for diabetic heart disease. *Cardiovascular Research*, *69*, 329–340. <https://doi.org/10.1016/j.cardiores.2005.09.017>
- Ron, D., & Walter, P. (2007). Signal integration in the endoplasmic reticulum unfolded protein response. *Nature Reviews. Molecular Cell Biology*, *8*, 519–529. <https://doi.org/10.1038/nrm2199>
- Sato, A., Asano, T., Isono, M., Ito, K., & Asano, T. (2014). Panobinostat synergizes with bortezomib to induce endoplasmic reticulum stress and ubiquitinated protein accumulation in renal cancer cells. *BMC Urology*, *14*, 71. <https://doi.org/10.1186/1471-2490-14-71>
- Schlossarek, S., Frey, N., & Carrier, L. (2014). Ubiquitin-proteasome system and hereditary cardiomyopathies. *Journal of Molecular and Cellular Cardiology*, *71*, 25–31. <https://doi.org/10.1016/j.yjmcc.2013.12.016>
- Sha, H., Sun, S., Francisco, A., Ehrhardt, N., Xue, Z., Liu, L., ... Qi, L. (2014). The ER-associated degradation adaptor protein Sel1L regulates LPL secretion and lipid metabolism. *Cell Metabolism*, *20*, 458–470. <https://doi.org/10.1016/j.cmet.2014.06.015>
- Shimizu, T., Shen, J., Fang, M., Zhang, Y., Hori, K., Trinidad, J. C., ... Masuda, S. (2017). Sulfide-responsive transcriptional repressor SqrR functions as a master regulator of sulfide-dependent photosynthesis. *Proceedings of the National Academy of Sciences of the United States of America*, *114*, 2355–2360.
- Sorrentino, A., Borghetti, G., Zhou, Y., Cannata, A., Meo, M., Signore, S., ... Rota, M. (2017). Hyperglycemia induces defective Ca²⁺ homeostasis in cardiomyocytes. *American Journal of Physiology - Heart and Circulatory Physiology*, *312*, H150–H161. <https://doi.org/10.1152/ajpheart.00737.2016>
- Stubbert, D., Prysazhna, O., Rudyk, O., Scotcher, J., Burgoyne, J. R., & Eaton, P. (2014). Protein kinase G 1α oxidation paradoxically underlies blood pressure lowering by the reductant hydrogen sulfide. *Hypertension*, *64*, 1344–1351. <https://doi.org/10.1161/HYPERTENSIONAHA.114.04281>
- Sun, Y., Tian, Z., Liu, N., Zhang, L., Gao, Z., Sun, X., ... Zhang, W. (2018). Exogenous H₂S switches cardiac energy substrate metabolism by regulating SIRT3 expression in db/db mice. *Journal of Molecular Medicine (Berlin, Germany)*, *96*, 281–299.
- Swatek, K. N., & Komander, D. (2016). Ubiquitin modifications. *Cell Research*, *26*, 399–422. <https://doi.org/10.1038/cr.2016.39>
- Untereiner, A. A., Fu, M., Modis, K., Wang, R., Ju, Y., & Wu, L. (2016). Stimulatory effect of CSE-generated H₂S on hepatic mitochondrial biogenesis and the underlying mechanisms. *Nitric Oxide*, *58*, 67–76. <https://doi.org/10.1016/j.niox.2016.06.005>
- Vidal, R. L., & Hetz, C. (2012). Crosstalk between the UPR and autophagy pathway contributes to handling cellular stress in neurodegenerative disease. *Autophagy*, *8*, 970–972. <https://doi.org/10.4161/Oauto.20139>
- Wallace, J. L., & Wang, R. (2015). Hydrogen sulfide-based therapeutics: exploiting a unique but ubiquitous gasotransmitter. *Nature Reviews. Drug Discovery*, *14*, 329–345. <https://doi.org/10.1038/nrd4433>
- Watkins, S. J., Borthwick, G. M., & Arthur, H. M. (2011). The H9C2 cell line and primary neonatal cardiomyocyte cells show similar hypertrophic responses in vitro. *In Vitro Cellular & Developmental Biology. Animal*, *47*, 125–131. <https://doi.org/10.1007/s11626-010-9368-1>
- Wiersma, M., Meijering, R. A. M., Qi, X. Y., Zhang, D., Liu, T., Hoogstra-Berends, F., ... Brundel, B. J. J. M. (2017). Endoplasmic reticulum stress is associated with autophagy and cardiomyocyte remodeling in experimental and human atrial fibrillation. *Journal of the American Heart Association*, *6*. <https://doi.org/10.1161/JAHA.117.006458>

- Willis, M. S., Schisler, J. C., Li, L., Rodriguez, J. E., Hilliard, E. G., Charles, P. C., & Patterson, C. (2009). Cardiac muscle ring finger-1 increases susceptibility to heart failure in vivo. *Circulation Research*, 105, 80–88. <https://doi.org/10.1161/CIRCRESAHA.109.194928>
- Willis, M. S., Schisler, J. C., Portbury, A. L., & Patterson, C. (2009). Build it up—Tear it down: Protein quality control in the cardiac sarcomere. *Cardiovascular Research*, 81, 439–448. <https://doi.org/10.1093/cvr/cvn289>
- Wu, D., Wang, J., Li, H., Xue, M., Ji, A., & Li, Y. (2015). Role of hydrogen sulfide in ischemia-reperfusion injury. *Oxidative Medicine and Cellular Longevity*, 2015, 186908.
- Wu, J., Tian, Z., Sun, Y., Lu, C., Liu, N., Gao, Z., ... Zhang, W. (2017). Exogenous H₂S facilitating ubiquitin aggregates clearance via autophagy attenuates type 2 diabetes-induced cardiomyopathy. *Cell Death & Disease*, 8, e2992. <https://doi.org/10.1038/cddis.2017.380>
- Xu, C., Bailly-Maitre, B., & Reed, J. C. (2005). Endoplasmic reticulum stress: Cell life and death decisions. *The Journal of Clinical Investigation*, 115, 2656–2664. <https://doi.org/10.1172/JCI26373>
- Xu, P., Duong, D. M., Seyfried, N. T., Cheng, D., Xie, Y., Robert, J., ... Peng, J. (2009). Quantitative proteomics reveals the function of unconventional ubiquitin chains in proteasomal degradation. *Cell*, 137, 133–145. <https://doi.org/10.1016/j.cell.2009.01.041>
- Yang, G., Wu, L., Jiang, B., Yang, W., Qi, J., Cao, K., ... Wang, R. (2008). H₂S as a physiologic vasorelaxant: Hypertension in mice with deletion of cystathionine γ -lyase. *Science*, 322, 587–590. <https://doi.org/10.1126/science.1162667>
- Yu, M., Salvador, L. A., Sy, S. K. B., Tang, Y., Singh, R. S. P., Chen, Q.-Y., ... Luesch, H. (2014). Largazole pharmacokinetics in rats by LC-MS/MS. *Marine Drugs*, 12, 1623–1640. <https://doi.org/10.3390/md12031623>
- Zhang, M., Perino, A., Ghigo, A., Hirsch, E., & Shah, A. M. (2013). NADPH oxidases in heart failure: Poachers or gamekeepers? *Antioxidants & Redox Signaling*, 18, 1024–1041. <https://doi.org/10.1089/ars.2012.4550>
- Zhao, D., & Yang, J. (2017). Insights for oxidative stress and mTOR signaling in myocardial ischemia/reperfusion injury under diabetes. *Oxidative Medicine and Cellular Longevity*, 2017, 2017, 6437467. <https://doi.org/10.1155/2017/6437467>

SUPPORTING INFORMATION

Additional supporting information may be found online in the Supporting Information section at the end of the article.

How to cite this article: Sun X, Zhao D, Lu F, et al. Hydrogen sulfide regulates muscle RING finger-1 protein S-sulfhydration at Cys⁴⁴ to prevent cardiac structural damage in diabetic cardiomyopathy. *Br J Pharmacol*. 2020;177:836–856. <https://doi.org/10.1111/bph.14601>